IMMUNOTHERAPY

Depletion of exhausted alloreactive T cells enables targeting of stem-like memory T cells to generate tumor-specific immunity

Simone A. Minnie[1], Olivia G. Waltner[1], Kathleen S. Ensbey[1], Nicole S. Nemychenkov[1], Christine R. Schmidt[1], Shruti S. Bhise[1], Samuel R. W. Legg[1], Gabriela Campoy[1], Luke D. Samson[1], Rachel D. Kuns[2], Ting Zhou[3], John D. Huck[3], Slavica Vuckovic[2], Danniel Zamora[4,5], Albert Yeh[1,4], Andrew Spencer[6,7,8], Motoko Koyama[1], Kate A. Markey[1,4], Steven W. Lane[2], Michael Boeckh[1,4,5], Aaron M. Ring[3], Scott N. Furlan[1,9], Geoffrey R. Hill[1,4]*

Some hematological malignancies such as multiple myeloma are inherently resistant to immune-mediated antitumor responses, the cause of which remains unknown. Allogeneic bone marrow transplantation (alloBMT) is the only curative immunotherapy for hematological malignancies due to profound graft-versus-tumor (GVT) effects, but relapse remains the major cause of death. We developed murine models of alloBMT where the hematological malignancy is either sensitive [acute myeloid leukemia (AML)] or resistant (myeloma) to GVT effects. We found that CD8$^+$ T cell exhaustion in bone marrow was primarily alloantigen-driven, with expression of inhibitory ligands present on myeloma but not AML. Because of this tumor-independent exhaustion signature, immune checkpoint inhibition (ICI) in myeloma exacerbated graft-versus-host disease (GVHD) without promoting GVT effects. Administration of post-transplant cyclophosphamide (PT-Cy) depleted donor T cells with an exhausted phenotype and spared T cells displaying a stem-like memory phenotype with chromatin accessibility present in cytokine signaling genes, including the interleukin-18 (IL-18) receptor. Whereas ICI with anti–PD-1 or anti–TIM-3 remained ineffective after PT-Cy, administration of a decoy-resistant IL-18 (DR-18) strongly enhanced GVT effects in both myeloma and leukemia models, without exacerbation of GVHD. We thus defined mechanisms of resistance to T cell–mediated antitumor effects after alloBMT and described an immunotherapy approach targeting stem-like memory T cells to enhance antitumor immunity.

INTRODUCTION

T cell exhaustion is a well-described driver of loss of immunosurveillance in many cancers, including hematological malignancies (*1*–*4*). The use of immunotherapies, such as immune checkpoint inhibition (ICI), has been a successful strategy to enhance antitumor effects in solid tumor settings as well as selected hematological malignancies (*5*–*7*). The importance of precursor exhausted and stem-like memory T cell subsets in generating a sustainable response to immunotherapies is becoming increasingly recognized, which has generated interest in targeting these populations directly (*8*–*10*). In hematological malignancies, particularly leukemias, allogeneic bone marrow transplantation (alloBMT) remains the only curative immunotherapy option (*11*). The curative potential of BMT is largely mediated by donor T cells recognizing recipient alloantigen comprising hematopoietic or tumor-specific antigens on the underlying malignancy, which is referred to as the graft-versus-tumor (GVT) effect (*12*). However, alloBMT is limited by donor T cell recognition of alloantigen on normal tissue, a process known as graft-versus-host disease (GVHD), as well as relapse of the original malignancy attributable to immune escape (*13*).

Studies where patients received PD-1 blockade after alloBMT have been associated with the exacerbation of GVHD, consistent with the role of PD-1 in suppressing alloreactive donor T cell function (*14*, *15*). Although there are a number of described mechanisms for immune escape after alloBMT (*16*), some hematological malignancies [e.g., myeloma (*13*, *17*)] are inherently resistant to GVT responses, and the cause of this remains unknown. Eliciting a strong GVT effect without inducing lethal GVHD likely requires modulation of the T cell repertoire such that highly alloreactive T cells are eliminated before initiating immunotherapy and/or immunotherapy selectively targeting tumor-specific T cells.

In this study, we first sought to understand why some hematological malignancies are resistant to GVT effects by developing preclinical models that were sensitive [acute myeloid leukemia (AML)] or resistant (myeloma) to GVT after alloBMT. Second, we used multiome single-cell sequencing techniques to phenotype T cells in the bone marrow (BM) microenvironment and identify pathways that could be targeted to improve GVT effects after alloBMT. We observed broad, alloantigen-induced CD8$^+$ T cell exhaustion that could be reduced with an immunosuppressant routinely used after alloBMT, cyclophosphamide (PT-Cy), which shifted the induction of CD8$^+$ T cell exhaustion to a malignancy-driven phenotype at myeloma relapse. Multiome sequencing demonstrated increased chromatin accessibility and RNA expression of the

[1]Clinical Research Division, Fred Hutchinson Cancer Center, Seattle, WA 98109, USA. [2]QIMR Berghofer Medical Research Institute, Brisbane, QLD 4006, Australia. [3]Department of Immunobiology, Yale School of Medicine, New Haven, CT 06519, USA. [4]Department of Medicine, University of Washington, Seattle, WA 98109, USA. [5]Vaccine and Infectious Disease Division, Fred Hutchinson Cancer Center, Seattle, WA 98109, USA. [6]Australian Center for Blood Diseases, Monash University/the Alfred Hospital, Melbourne, VIC 3004, Australia. [7]Malignant Haematology and Stem Cell Transplantation, the Alfred Hospital, Melbourne, VIC 3004, Australia. [8]Department of Clinical Haematology, Monash University, Melbourne, VIC 3800, Australia. [9]Department of Pediatrics, University of Washington, Seattle, WA 98105, USA.
*Corresponding author. Email: grhill@fredhutch.org

interleukin-18 (IL-18) receptor on stem-like memory CD8$^+$ T cells after PT-Cy. Last, we tested several immunotherapies after PT-Cy and found that although ICI did not induce lethal GVHD, it also failed to enhance GVT effects. Conversely, an IL-18 cytokine mimetic (DR-18) facilitated potent antitumor responses in both myeloma and leukemia without markedly exacerbating GVHD.

RESULTS

Graft-versus-myeloma effects are subverted after alloBMT

To determine potential factors underlying the resistance of patients with myeloma to GVT effects, we generated preclinical murine models of transplantation for primary AML and myeloma that we found to be GVT-sensitive and GVT-resistant, respectively. To achieve this, we developed a system of allogeneic BMT where C57Bl/6 recipients are transplanted with BM and T cell grafts from minor MHC (major histocompatibility complex)–mismatched C3H.SW donors (alloBMT) or syngeneic C57Bl/6 donors (synBMT). We used a green fluorescent protein (GFP)–expressing MLL-AF9–driven leukemia that allows for monitoring of tumor cells in peripheral blood and Vk*MYC myeloma that secretes immunoglobulin G (IgG), which can be monitored by serum protein electrophoresis as an M-band (albumin/gamma ratio) that is a hallmark of clinical disease. In mice bearing MLL-AF9–driven AML, recipients of allogeneic grafts had significantly reduced circulating leukemia cells and a reduced relapse-related mortality compared with synBMT, confirming an allogeneic graft-versus-leukemia (GVL) effect (Fig. 1, A and B). Mice with late leukemia-related deaths in the alloBMT group succumbed to marrow failure, consistent with systemic immune control but local escape from GVL effects in the BM. In contrast, ineffective graft-versus-myeloma (GVM) responses were seen in Vk*MYC myeloma–bearing recipients, with no significant difference in the rate of myeloma growth as determined by M-band progression. Furthermore, competing risk analysis revealed that there was a significantly increased risk of GVHD in alloBMT recipients compared with synBMT that outweighed any potential GVM effects (Fig. 1, C and D). Thus, although an effective GVT response could be generated after alloBMT against AML, this was subverted in MM-bearing recipients, an observation that recapitulates clinical data demonstrating that myeloma is largely resistant to GVT effects (*17*). Mechanisms underpinning this GVT resistance could be broadly applicable clinically, because some patients with AML have reduced GVT sensitivity relative to highly sensitive malignancies (e.g., chronic myeloid leukemia) (*18*).

Donor CD8$^+$ T cells undergo exhaustion in response to allogeneic rather than tumor antigens after alloBMT

To determine the mechanisms responsible for the ineffective GVM response after alloBMT, we performed immune phenotyping of CD8$^+$ T cells in the BM between 2 and 8 weeks after transplantation using flow cytometry. These experiments were performed in the absence of myeloma (MM-free) to control for the effects of concurrent myeloma on CD8$^+$ T cell function after BMT (*3*). We focused on CD8$^+$ T cells initially because GVHD in this model is primarily MHC class I dependent, and we have previously shown that CD8$^+$ T cells are crucial to long-term myeloma-specific immunity after autologous BMT (*19*). We used multidimensional *t*-distributed stochastic neighbor embedding (t-SNE) analysis of our flow cytometry data and observed differential clustering of allogeneic and syngeneic CD8$^+$ T cells by 2 weeks after transplant (Fig. 2A). This phenotype persisted through 8 weeks after transplant. We noted a significant expansion of CD8$^+$ T cells 2 to 4 weeks after transplant in alloBMT recipients, which were predominately effector memory T cells (CD44$^+$CD62L$^-$, T_{EM}; Fig. 2, B and C). Conversely, synBMT recipients had equivalent CD4$^+$ and CD8$^+$ T cell expansion with higher frequencies of central memory (CD44$^+$CD62L$^+$, T_{CM}) versus T_{EM} CD8$^+$ T cells (Fig. 2, B and C). Most CD8$^+$ T cells expressed TIGIT, PD-1, and TIM-3 early after alloBMT, and both PD-1 and TIGIT expression persisted long term (Fig. 2D). DNAM-1 expression was maintained on a proportion of CD8$^+$ T cells after alloBMT, suggesting that these T cells were either activated or at an early stage of exhaustion (Fig. 2A) (*3*, *20*). Expansion of these alloreactive CD8$^+$ T_{EM} cells after alloBMT would be expected to result in enhanced tumor control relative to synBMT, but this was only seen in response to AML, suggesting that the subversion of GVM may reflect tumor-related differences either intrinsic to myeloma or related to differential effects exerted by myeloma (versus AML) on the tumor microenvironment (TME). We therefore investigated the expression of relevant inhibitory receptor ligands on the cell surface of Vk12653 myeloma and MLL-AF9 AML. We noted differential expression of both CD155 and PD-L1, the ligands for TIGIT and PD-1, respectively, on Vk*MYC compared with MLL-AF9 (Fig. 2E). This expression of CD155 on malignant cells has previously been demonstrated to infer resistance to T cell–dependent antitumor immunity (*21*). Furthermore, TIGIT has a much higher affinity than DNAM-1 for CD155 and will outcompete for ligand binding even if DNAM-1 expression is maintained on CD8$^+$ T cells (*22*). Therefore, donor CD8$^+$ T cells expressing high levels of TIGIT$^+$ and PD-1$^+$ in response to alloantigen were putatively inactivated via interaction with cognate inhibitory receptor ligands expressed by myeloma.

TIGIT inhibition does not enhance GVM after alloBMT

Because CD155 and PD-L1 expression on myeloma cells is a potential mechanism of immune escape after alloBMT, we explored whether these pathways could be targeted therapeutically to generate GVM effects. We have previously demonstrated that PD-1 or TIGIT blockade after synBMT significantly improved myeloma-specific immunity (*3*). PD-1 inhibition after alloBMT can exacerbate GVHD in both preclinical models and clinical practice (*15*, *23*–*25*). To examine whether TIGIT inhibition would affect GVHD and/or GVM, we treated MM-bearing recipients with TIGIT blocking antibodies. Recipients treated with an Fc-enabled (i.e., live) 4B1-G2a clone, αTIGIT-G2a, after transplant had significantly enhanced mortality compared with isotype control (cIg)–treated mice (Fig. 2F). This was associated with an increase in GVHD clinical scores and GVHD-induced mortality, without an associated improvement in the GVM effect (Fig. 2, G to I).

We next tested the Fc-dead anti-TIGIT G1-D265A clone (αTIGIT-G1) that does not deplete TIGIT-expressing regulatory T cells and hypothesized that exacerbation of GVHD would be less severe than the Fc-enabled TIGIT (*26*, *27*). Mice treated with αTIGIT-G1 from 3 weeks after alloBMT had similar overall survival compared to isotype-treated mice (fig. S1A). GVHD, myeloma burden, and myeloma progression were similar between αTIGIT-G1– and cIg-treated mice (fig. S1, B to D). Therefore, TIGIT inhibition was not sufficient to generate GVM responses after alloBMT.

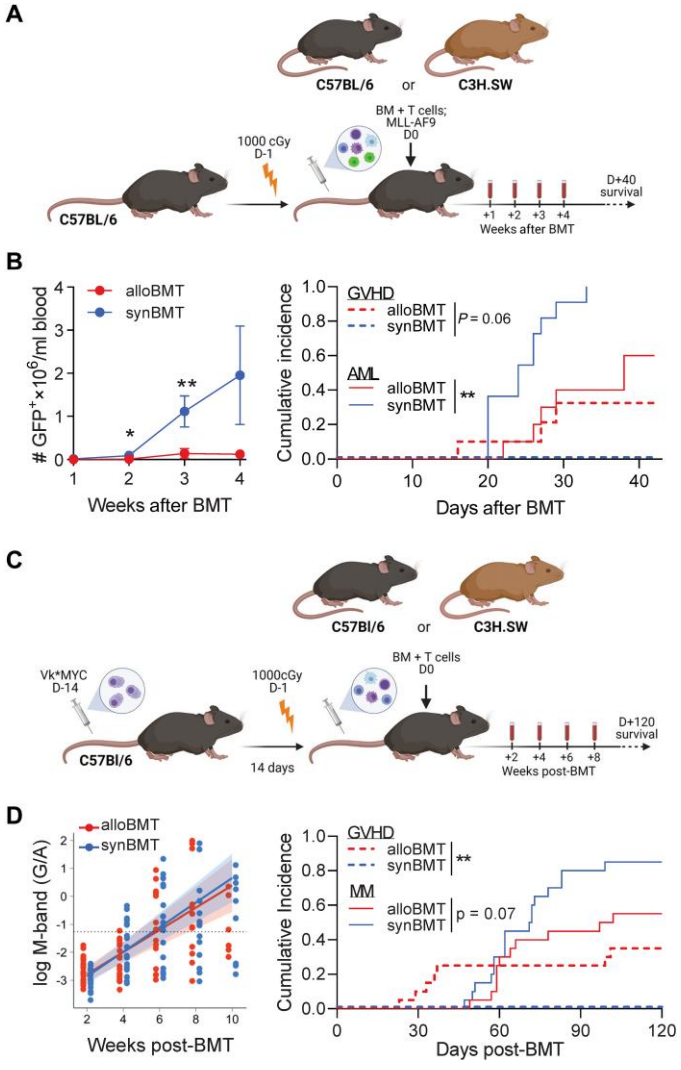

Fig. 1. GVT effects were subverted after alloBMT in myeloma-bearing, but not leukemia-bearing, recipients. C57Bl/6 (B6) recipients injected with Vk*MYC myeloma (MM-bearing; D−14) or MLL-AF9 (AML-bearing; D0) were lethally irradiated and transplanted with 5×10^6 BM with 0.5×10^6 $CD4^+$ + 0.5×10^6 $CD8^+$ T cells from B6 (synBMT) or C3H.SW (alloBMT) donors. (**A**) Experimental schematic. (**B**) AML-bearing recipients were bled weekly to quantify the total number of circulating GFP^+ AML cells, and competing risk analysis was performed to determine risk of death due to AML or GVHD. n = 11 per group from two experiments. Mann-Whitney U test for AML burden. (**C**) Experimental schematic. (**D**) MM-bearing recipients were monitored for tumor burden using M-band (G/A). M-bands were modeled to calculate a predictive rate of tumor growth (solid line), with shaded confidence intervals and M-band relapse threshold shown as dotted line. Competing risk analysis was performed to determine risk of death due to myeloma (MM) or graft-versus-host disease (GVHD). n = 20 per group from three experiments. *P < 0.05 and **P < 0.01.

This is in contrast to previous data demonstrating that blockade of myeloma-induced TIGIT expression on $CD8^+$ T cells could induce potent myeloma immunity in a synBMT model (where alloantigen is absent) (*3*). This led us to investigate whether the expression of inhibitory receptors on $CD8^+$ T cells was generated by $CD8^+$ T cell recognition of malignancy-derived antigens or broadly by recipient alloantigens after alloBMT.

Myeloma itself does not drive T cell exhaustion after alloBMT

To determine the relative contribution of tumor versus allogeneic antigens to $CD8^+$ T cell exhaustion, we analyzed $CD8^+$ T cells in the BM of myeloma-bearing recipients (MM-bearing) or control mice that were transplanted in the absence of myeloma (MM-free) at 8 weeks after alloBMT, a time point of active myeloma progression in the MM-bearing cohort. We noted only a small increase in PD-1 and TIM-3 expression and reduced DNAM-1 expression in MM-bearing versus MM-free controls (Fig. 3, A and B). In particular, an increase in the frequency of $CD101^+CD38^+CD8^+$ T cells was seen in MM-bearing compared with MM-free mice (Fig. 3B), a phenotype that is usually associated with dysfunctional, terminally exhausted T cells (*3*, *28*). Nonetheless, $CD8^+$ T cells from MM-bearing mice did not have alterations in interferon-γ (IFN-γ) or tumor necrosis factor (TNF) production upon ex vivo restimulation [with phorbol 12-myristate 13-acetate (PMA)/ionomycin] after alloBMT compared with MM-free mice (Fig. 3C), likely due to the relatively low frequency of $CD38^+CD101^+$ cells within the $CD8^+$ T cell compartment. Together, these data demonstrate that cytokine production by BM $CD8^+$ T cells was not adversely affected by the presence of myeloma after alloBMT. Similar analyses in AML-bearing mice also demonstrated a significant increase in PD-1 expression and a concurrent decrease in DNAM-1 expression compared with AML-free mice (Fig. 3, D and E). However, in AML-bearing mice the overall frequency of IFN-γ^+ $CD8^+$ T cells was reduced (Fig. 3F), indicating that tumor-induced $CD8^+$ T cell dysfunction occurred in this leukemia model. The absence of exaggerated $CD8^+$ T cell exhaustion in mice with relapsed myeloma after alloBMT confirms that the main driver of T cell exhaustion in this setting is alloantigen rather than tumor-specific antigen, potentially explaining why TIGIT blockade exacerbated GVHD without promoting GVM (Fig. 2, F to I).

Post-transplant cyclophosphamide attenuates alloantigen-induced $CD8^+$ and $CD4^+$ T cell exhaustion in the BM after alloBMT

We next investigated whether we could eliminate highly activated, alloreactive T cells to preserve T cell subsets that could be safely harnessed to improve GVT responses in the BM after alloBMT. To achieve this, we treated alloBMT recipients with a currently used GVHD prophylaxis strategy, post-transplant cyclophosphamide (PT-Cy), that strongly attenuates alloreactive T cell responses and GVHD. We first assessed T cell phenotypes in the BM 14 days after transplantation in MM-free mice to generate a dataset that could be broadly interpreted independent of specific tumor-induced phenotypes. We performed single-cell sequencing on sorted T cells from BM with the 10x Genomics Multiome platform to measure concurrent changes in gene expression (RNA sequencing) and chromatin accessibility [ATAC (assay for transposase-accessible chromatin) sequencing]. Unsupervised clustering on the basis of weighted nearest neighbor algorithms identified eight clusters within $CD8^+$ (fig. S2) and five clusters within $CD4^+$ (fig. S3) T cells. Clusters were annotated based on all differentially expressed genes in each cluster (data files S1 and S2), and we have highlighted key genes associated with each cluster in $CD8^+$ (Fig. 4A) and $CD4^+$ (Fig. 4B) T cells.

In untreated alloBMT recipients, $CD8^+$ T cells highly expressed genes associated with T cell exhaustion, whereas those in PT-Cy–

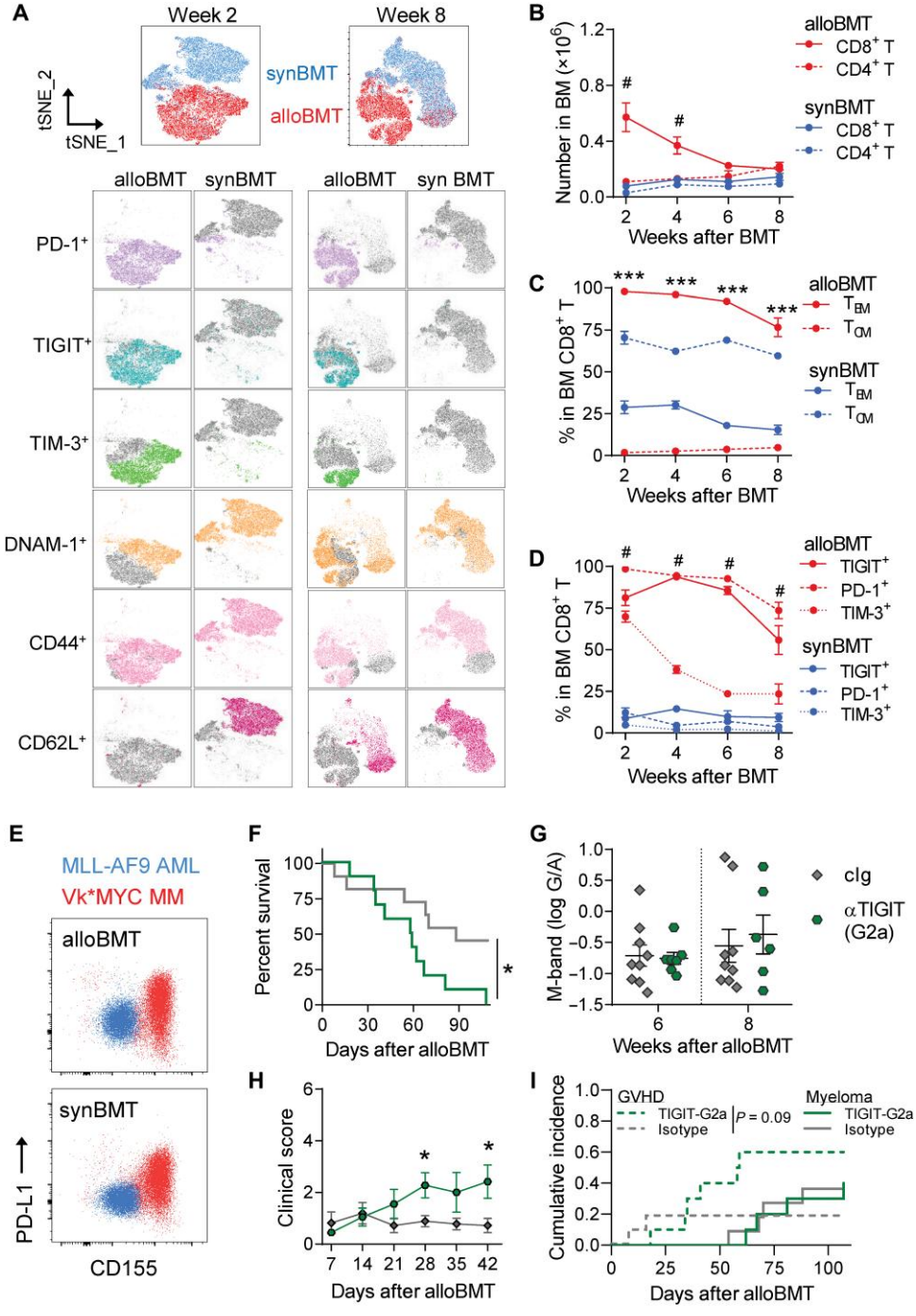

Fig. 2. Alloantigen-driven inhibitory receptor expression corresponded with ligand expression on myeloma, and blockade exacerbated GVHD. B6 recipients were transplanted with 5×10^6 BM with 0.5×10^6 $CD4^+$ + 0.5×10^6 $CD8^+$ T cells from B6 (synBMT) or C3H.SW (alloBMT) donors. (**A** to **D**) BM was harvested, and T cells were phenotyped at 2, 4, 6, and 8 weeks after transplant ($n = 3$ to 8 from one or two experiments). $^{\#}P < 0.05$ when alloBMT and synBMT were compared using two-way ANOVA with Tukey's multiple comparisons test. (A) t-SNE analysis identified $CD8^+$ T cell clusters based on PD-1, TIGIT, TIM-3, DNAM-1, CD44, and CD62L expression at 2 and 8 weeks after transplant ($n = 3$ to 5). (B) $CD4^+$ and $CD8^+$ T cell numbers. (C) Frequency of effector $CD8^+$ T cells ($CD44^+CD62L^-$, T_{EM}) and central memory T cells ($CD44^+$-$CD62L^+$, T_{CM}). (D) Frequency of $TIGIT^+$, $PD\text{-}1^+$, and $TIM3^+$ $CD8^+$ T cells. (**E**) FACS plots of PD-L1 and CD155 expression on Vk12653 (red) and MLL-AF9 (blue). (**F** to **I**) Recipients were treated with 100 μg per mouse of anti-TIGIT (clone G2a; αTIGIT-G2a) or mIgG2a isotype control (cIg) twice a week from 2 to 6 weeks after transplant. (F) Median overall survival analyzed with log-rank test, (G) M-band (log gamma/albumin) at 6 and 8 weeks after alloBMT, (H) clinical score, and (I) competing risk analysis ($n = 10$ per group from two experiments). Data represent means ± SEM. Two-way ANOVA with Tukey's multiple comparisons test. $^*P < 0.05$ and $^{***}P < 0.001$.

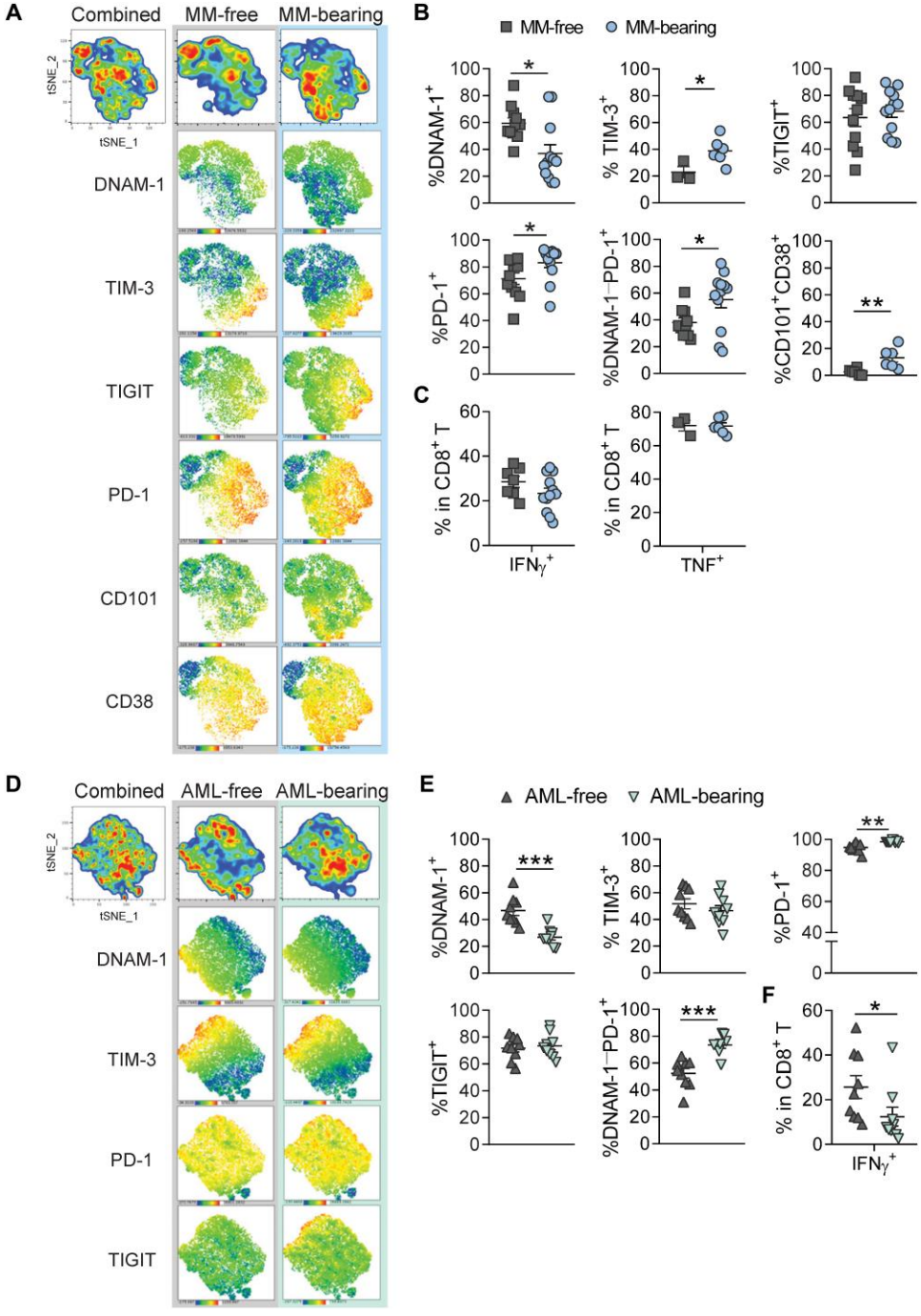

Fig. 3. CD8⁺ T cell exhaustion was primarily driven by alloantigen, and not tumor antigen, after alloBMT. B6 recipients were transplanted with 5×10^6 BM with 0.5×10^6 $CD4^+$ + 0.5×10^6 $CD8^+$ T cells from C3H.SW (alloBMT) donors. (**A** to **C**) Myeloma-bearing (MM-bearing) or naïve (MM-free) recipients were euthanized at 8 weeks after transplant, and BM was harvested to assess $CD8^+$ T cell phenotype. (A) Representative t-SNE analysis of PD-1, TIGIT, TIM-3, DNAM-1, CD101, and CD38 expression and (B) frequency of DNAM-1^+, TIM-3^+, $TIGIT^+$, PD-1^+, DNAM-1^-PD-1^+, and $CD101^+CD38^+$ cells within $CD8^+$ T cells. (C) Frequency of IFN-γ– and TNF-expressing cells within $CD8^+$ T cells after PMA/ionomycin restimulation (n = 11 or 12 per group from two experiments; TNF and TIM-3 n = 3 to 6 per group from one experiment). (**D** to **F**) MLL-AF9–bearing (AML-bearing) or naïve (AML-free) mice were euthanized 4 weeks after transplant, and BM was harvested to assess $CD8^+$ T cell phenotype. (D) t-SNE analysis of PD-1, TIGIT, TIM-3, and DNAM-1 expression and (E) frequency of DNAM-1^+, TIM-3^+, PD-1^+, $TIGIT^+$, and DNAM-1^-PD-1^+ cells within $CD8^+$ T cells. (F) Frequency of IFN-γ–expressing cells within $CD8^+$ T cells after PMA/ionomycin restimulation (n = 9 per group from two experiments). Data represent means ± SEM. Mann-Whitney U test or Student's t test was used for numerical values. *P < 0.05, **P < 0.01, and ***P < 0.001.

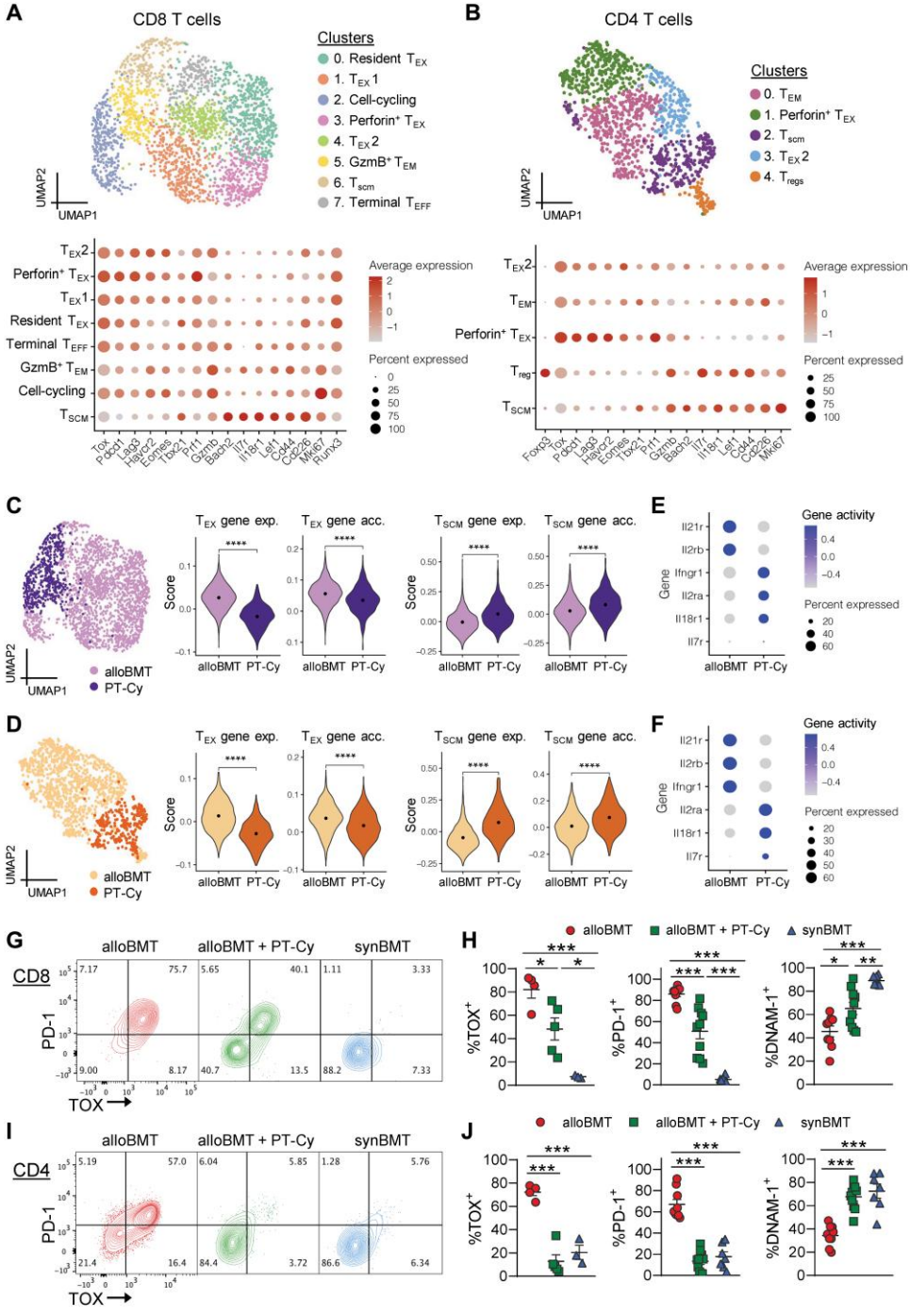

Fig. 4. PT-Cy reduced alloreactive T cell exhaustion and enhanced stemness in BM. B6 recipients were transplanted with 5×10^6 BM with 0.5×10^6 $CD4^+$ + 0.5×10^6 $CD8^+$ T cells from C3H.SW donors (alloBMT) or B6 donors (synBMT). Some alloBMT recipients were treated with cyclophosphamide (50 mg/kg) on D+3 and D+4 after transplantation (alloBMT + PT-Cy). Mice were euthanized 14 days after transplant, and BM was harvested and pooled from four mice per group. (**A** to **F**) $CD8^+$ and $CD4^+$ T cells were sort-purified from BM of alloBMT and alloBMT + PT-Cy recipients, and nuclei were processed for 10x Genomics Multiome sequencing. (A) WNN embedding of combined ATAC and RNA data of $CD8^+$ cells colored by cluster (top) then annotated using $CD8^+$ T cell–specific markers (bottom). (B) $CD4^+$ T cells clustered and annotated in a manner analogous to (A). (C) Embedding in (A) colored by experimental group (left). Centered and scaled cumulative gene expression (exp.) and gene accessibility (acc.; using gene activity score) of T_{EX} and T_{SCM} genes in $CD8^+$ T cells by experimental group (right). Wilcoxon rank sum test. (D) Embedding in (B) colored by experimental group (left). Centered and scaled cumulative gene expression and gene accessibility of T_{EX} and T_{SCM} genes in $CD4^+$ T cells by experimental group (right). Wilcoxon rank sum test. (E and F) Gene accessibility scores of key cytokine receptor genes by experiment group in (E) $CD8^+$ T cells and (F) $CD4^+$ T cells. (**G** to **J**) Representative flow cytometry plots of PD-1 versus TOX expression in $CD8^+$ and $CD4^+$ conventional ($FoxP3^-$) T cells. (H) Frequency of TOX^+, PD-1^+, and DNAM-1^+ within $CD8^+$ T cells (J) and $CD4^+$ conventional T cells ($n = 7$ to 10 per group from two experiments, TOX $n = 3$ to 5 per group from one experiment). Data represent means ± SEM. One-way ANOVA with Tukey's multiple comparisons test. *$P < 0.05$, **$P < 0.01$, ***$P < 0.001$, and ****$P < 0.0001$.

treated alloBMT recipients had higher expression of stem-like memory gene signatures (Fig. 4C and fig. S4) (*9*, *29*). When T cells were unbiasedly clustered, most CD8$^+$ T cells from PT-Cy–treated recipients were within a cluster (number 6) that included stem-like memory cells (T_{SCM}) characterized by *Bach2*, *Ly6a* (encoding sca-1), *Il7r*, *Il18r1*, *Cd226*, and absence of *Pdcd1* (Fig. 4A). These changes in gene expression were mirrored by changes in chromatin accessibility: We observed a similar skewing toward stem-like signatures measured by gene accessibility scores (Fig. 4C). Together, these findings confirm a fundamental change in the phenotype of CD8$^+$ T cells surviving PT-Cy. Analogous to the CD8$^+$ T cell compartment, CD4$^+$ T cells from alloBMT recipients were enriched for the same exhaustion signature, whereas those in PT-Cy–treated recipients were largely enriched for a T_{SCM} signature (Fig. 4D and fig. S5). Furthermore, chromVAR analysis highlighted motifs associated with exhaustion [i.e., NR4A1 (*30*) and NFATC (*31*)] in T cells from control alloBMT recipients, whereas T cells from PT-Cy–treated alloBMT recipients had motifs associated with stemness [i.e., TCF7 (*32*) and KLF] (fig. S6). To identify functional relevance of PT-Cy–driven epigenetic changes, we measured chromatin accessibility in key cytokine receptor genes and noted that *Il18r1* (IL-18R), *Il2ra* (IL-2Rα), and *Il7r* (IL-7R) demonstrated increased gene activity scores after PT-Cy in both CD8$^+$ and CD4$^+$ T cells (Fig. 4, E and F).

Last, we corroborated our sequencing data of BM T cells from alloBMT recipients with and without PT-Cy with flow cytometry at the same time point, including synBMT recipients as a baseline for any immune effects of transplantation itself. We confirmed that CD8$^+$ T cells had an exhausted phenotype after alloBMT, characterized by expression of high levels of TIGIT, PD-1, TOX, and TIM-3 proteins, whereas syngeneic T cells were DNAM-1$^+$ without inhibitory ligand expression (Fig. 4, G and H, and fig. S7A). CD8$^+$ T cells from PT-Cy–treated alloBMT recipients had significantly increased DNAM-1 and reduced TIGIT, PD-1, and TOX expression, with a phenotype intermediate to T cells from alloBMT recipients without PT-Cy and recipients of synBMT (where alloantigen was absent). PT-Cy treatment did not abrogate granzyme B production by CD8$^+$ T cells, as determined by both RNA and protein expression (figs. S4 and S7A). The marked effect of PT-Cy on the CD4$^+$ T cell compartment was also confirmed by flow cytometry such that the CD4$^+$ T cell exhaustion signature in FoxP3$^-$ conventional CD4$^+$ T cells from PT-Cy–treated recipients was largely indistinguishable from synBMT recipients, consistent with a dominant effect on class II–dependent alloreactivity (Fig. 4, I and J, and fig. S7B). Together, these data demonstrate that PT-Cy reduced the frequency of alloreactive, exhausted T cells in the BM of alloBMT recipients and instead enriched for T_{SCM} populations, offering a potential platform on which to subsequently generate tumor-specific responses.

PT-Cy is permissive of myeloma-driven T cell exhaustion after alloBMT

We next treated MM-bearing recipients with PT-Cy after alloBMT and compared myeloma growth and survival with untreated recipients to determine whether the loss of putative alloreactive T cells in the BM affected the control of myeloma. PT-Cy resulted in early myeloma cytoreduction with reduced M-bands at 4 weeks after alloBMT that was also seen in recipients of T cell–depleted BM (Fig. 5, A and B), consistent with the expected cytoreduction mediated by cyclophosphamide. However, this PT-Cy effect was not durable, because there was a subsequent increase in myeloma progression as determined by M-band 8 weeks after alloBMT in PT-Cy–treated recipients (Fig. 5A). Consistent with this effect, total T cell numbers were also concurrently reduced by PT-Cy at D+14 and D+21 after alloBMT (fig. S8, A and B). Together, these data suggest that direct myeloma cytoreduction partially counteracts the loss of alloreactive T cells mediating GVT effects after PT-Cy.

Having established that PT-Cy reduced alloantigen-induced T cell exhaustion, enriched for a T_{SCM} phenotype, and did not significantly reduce overall survival, we next sought to determine whether the presence of myeloma in the BM would alter T cell phenotypes in PT-Cy–treated alloBMT recipients with relapsed disease. We analyzed CD8$^+$ and CD4$^+$ T cells at 7 weeks after transplant from the BM of MM-bearing and MM-free allograft recipients that were treated with and without PT-Cy. In untreated recipients, there was high expression of TIGIT, TIM-3, and TOX on CD8$^+$ T cells regardless of whether the mice were MM-free or had active myeloma, indicative of broad alloantigen-driven T cell exhaustion (Fig. 5, C, F, and G). In MM-free PT-Cy–treated recipients, most CD8$^+$ T cells were DNAM-1$^+$TIGIT$^-$ and did not express TOX or TIM-3 (Fig. 5, C, F, and G), consistent with maintained depletion of exhausted alloreactive T cells observed at D+14 (Fig. 4). However, in MM-bearing PT-Cy–treated recipients, most CD8$^+$ T cells were DNAM-1$^-$TIGIT$^+$ with high expression of TOX and TIM-3 (Fig. 5, C, F, and G), consistent with the onset of myeloma-driven T cell exhaustion. Even at this late time point, the reduction in total numbers of CD4$^+$ and CD8$^+$ T cells in PT-Cy–treated recipients was maintained (Fig. 5D). In PT-Cy–treated MM-free recipients, there was an increase in CD8$^+$ central memory (T_{CM}; CD44$^+$CD62L$^+$) and a decrease in terminal effector (T_{EFF}; CD44$^-$CD62L$^-$) T cells, consistent with maintenance of the memory populations we identified at earlier time points (Figs. 4C and 5E). Increased expression of TOX and inhibitory receptors, including the terminal exhaustion markers TIM-3 and CD101, on effector cells in MM-bearing compared with MM-free PT-Cy–treated recipients is consistent with the expansion of exhausted, putatively myeloma-specific T cells, a phenotype observed at MM progression after synBMT (*3*). Therefore, PT-Cy effectively eliminated alloantigen-driven CD8$^+$ T cell exhaustion and enabled exhaustion to instead be driven by myeloma. Although there was a marked effect on CD4$^+$ T cells after PT-Cy, there were only subtle differences in this compartment in MM-free versus MM-bearing recipients, including an increase in TOX but not TIGIT or TIM-3 expression (Fig. 5, C, H, and I). This finding is unsurprising given the high expression of MHC class I and absence of MHC class II on Vk*MYC myeloma cells (*19*). Last, we confirmed the presence of tumor-driven T cell exhaustion after PT-Cy in the MLL-AF9 AML model. We observed an increased frequency of TIM-3$^+$CX3CR1$^-$ CD8$^+$ T cells at 3 weeks after transplant in mice with relapsed AML compared with AML-free recipients after PT-Cy (fig. S9). Expression of CX3CR1 was used to exclude transitionary effector cells that contaminate the TIM-3$^+$ population at earlier time points in tumor progression (*33*).

Agonist immunotherapies are required to promote GVM after PT-Cy

Given the presence of myeloma-driven expression of inhibitory receptors on CD8$^+$ T cells at relapse after PT-Cy, we tested the anti-myeloma efficacy of ICI in PT-Cy–treated alloBMT recipients (Fig. 6A). We administered ICIs, either anti–PD-1 or anti–TIM-3,

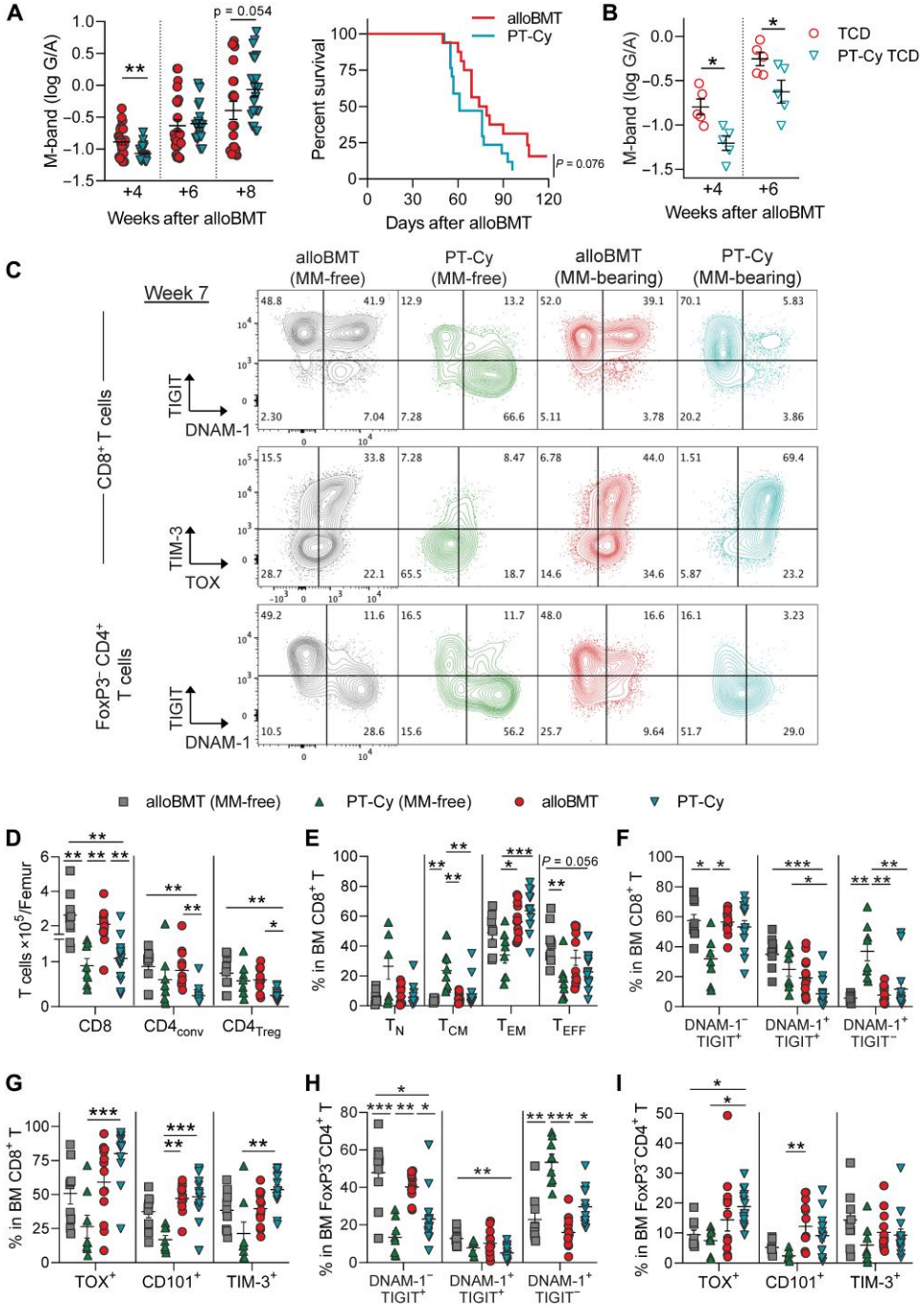

Fig. 5. PT-Cy enabled the generation of myeloma-driven CD8⁺ T cell exhaustion. B6 MM-bearing recipients were transplanted with 5×10^6 BM with 0.5×10^6 $CD8^+$ and 0.5×10^6 $CD4^+$ T cells from C3H.SW donors. (**A**) MM-bearing recipients of T cell–replete grafts were untreated (alloBMT) or administered cyclophosphamide (50 mg/kg) on D+3 and D+4 (PT-Cy) and monitored for myeloma burden using M-band (log G/A; $n = 24$ from four experiments; Mann-Whitney U test) and survival ($n = 17$ from three experiments; log-rank test). (**B**) MM-bearing recipients of T cell–depleted BM grafts (TCD) were treated as above and monitored for M-band ($n = 5$ from one experiment; Student's t test). (**C** to **I**) MM-bearing and MM-naïve recipients were treated as above, and BM was harvested at 7 weeks after transplant for immunophenotyping using flow cytometry ($n = 8$ to 14 from two experiments). (C) Representative contour plots. (D) $CD8^+$, conventional $CD4^+$ ($FoxP3^-$), and regulatory $CD4^+$ T cell enumeration per femur. (E) Frequency of naïve T (T_N; $CD44^-CD62L^+$), central memory T (T_{CM}; $CD44^+CD62L^+$), effector memory T (T_{EM}; $CD44^+CD62L^-$), and effector T (T_{EFF}; $CD44^-CD62L^-$); (F) DNAM-1– and TIGIT-expressing cells; and (G) TOX^+, $CD101^+$, and $TIM\text{-}3^+$ cells within $CD8^+$ T cells. (H) Frequency of DNAM-1– and TIGIT-expressing cells and (I) TOX^+, $CD101^+$, and $TIM\text{-}3^+$ cells within conventional $CD4^+$ T cells. Data represent means ± SEM. One-way ANOVA with Tukey's multiple comparisons test or Kruskal-Wallis test with Dunn's multiple comparisons test. *$P < 0.05$, **$P < 0.01$, and ***$P < 0.001$

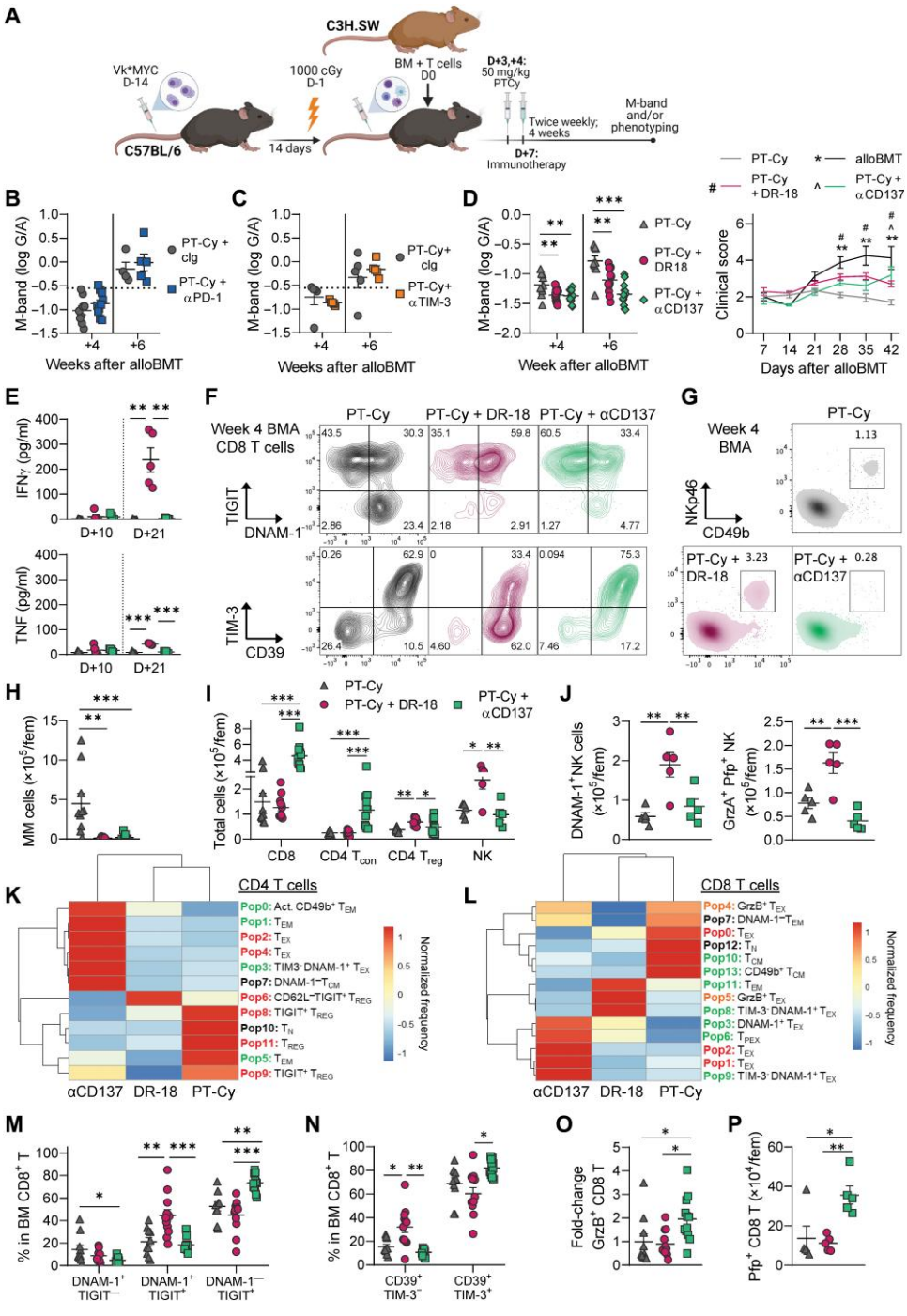

Fig. 6. Agonist immunotherapy promoted GVM after PT-Cy. B6 MM-bearing recipients were transplanted with 5×10^6 BM and 1×10^6 $CD8^+$ and 1×10^6 $CD4^+$ T cells from C3H.SW donors. Recipients were administered cyclophosphamide (50 mg/kg) on D+3 and D+4 and then either a vehicle control or immunotherapy from D+7 for 4 weeks. (**A**) Experimental design. (**B**) M-band of recipients treated with rIgG2a (PT-Cy) or anti–PD-1 (PT-Cy + αPD-1). $n = 10$ from two experiments at 4 weeks; $n = 5$ from one experiment at 6 weeks. (**C**) M-band of recipients treated with rIgG2a (PT-Cy) or anti–TIM-3 (PT-Cy + αTIM-3). $n = 5$ from one experiment. (**D** to **P**) MM-bearing recipients were treated with PBS (PT-Cy), or 8 μg per dose of DR-18 (PT-Cy + D−18), or 100 μg per dose of anti-CD137 (PT-Cy + αCD137). BM aspirates (BMA) were performed at 4 weeks after transplant from one femur. Mice were then euthanized at 6 weeks after alloBMT, and BM from both femurs was harvested. $n = 10$ to 12 from two experiments unless otherwise stated. (D) M-band at 4 and 6 weeks after alloBMT and GVHD clinical (including alloBMT mice not treated with PT-Cy; $n = 5$ from one experiment). (E) IFN-γ and TNF (pg/ml) in serum at D+10 and D+21 after alloBMT ($n = 5$ from one experiment). (F) Concatenated contour plots of TIGIT versus DNAM-1, and TIM-3 versus CD39 expression on $CD8^+$ T cells from BM aspirates (representative of two experiments). (G) Concatenated density plots of NK cell frequency ($NKp46^+$ $CD49b^+$) within white blood cells from BM aspirates. (H) Myeloma and (I) T and NK cell total numbers per femur at week 6. (J) Number of DNAM-1^+ and granzyme A^+ perforin$^+$ ($GrzA^+Pfp^+$) NK cells ($n = 5$ per group from one experiment). (K to L) FlowSOM clustering was performed on concatenated (K) $CD4^+$ and (L) $CD8^+$ T cells at week 6 after transplant. Heatmaps depict relative frequencies of populations across treatment groups. Populations are colored on the basis of expected antitumor properties. Green, activated effector or memory populations; orange, cytolytic; red, exhausted/suppressive; and black, unknown. (M) Frequency of DNAM-1– and TIGIT-expressing and (N) CD39- and TIM-3–expressing cells within $CD8^+$ T cells at week 6. (O) Fold change in granzyme B ($GrzB^+$) expression on $CD8^+$ T cells and (P) total number of perforin-expressing (Pfp^+; $n = 5$ per group from one experiment) $CD8^+$ T cells at week 6 after transplant. Data represent means ± SEM. One-way ANOVA with Tukey's multiple comparisons test or Kruskal-Wallis test with Dunn's multiple comparisons test. $^*P < 0.05$, $^{**}P < 0.01$, and $^{***}P < 0.001$.

from D+7 for 4 weeks and observed no reduction in myeloma burden in ICI-treated mice (Fig. 6, B and C). For ICI to be effective, there must be an appropriate ratio of ICI-responsive T cells to tumor burden (*34*). PT-Cy resulted in reduced expression of inhibitory receptors (Fig. 4C) in the context of strongly reduced overall T cell numbers (fig. S8) at the time point where ICI was administered. These data suggest that immunotherapies targeting a "brake" on T cell function were unlikely to drive effective anti-myeloma responses in this setting. To that end, we next investigated two immunotherapies with known direct agonist activity, decoy-resistant IL-18 [DR-18 (*35*)] and anti-CD137 [4-1BB (*19*)]. DR-18 is a synthetic cytokine that is resistant to the IL-18 binding protein, which usually counteracts the proinflammatory effects of native IL-18 in vivo. In solid tumor models, DR-18 promotes IFN-γ–dependent, $CD8^+$ T cell–mediated antitumor responses (*35*). We were especially interested in this agonist because IL-18R gene expression and

chromatic accessibility was increased in both CD4$^+$ and CD8$^+$ T_{SCM} cells (Fig. 4, A, B, E, and F). Furthermore, IL-18R is known to be expressed on human memory T cells, and we have confirmed expression of IL-18R on CD4$^+$ and CD8$^+$ T_{SCM} in patients who underwent allogeneic stem cell transplantation (fig. S10) (*36*). The CD137 agonist was chosen because of known anti-myeloma activity in other preclinical models, and CD137 (*Tnfrsf9*) was broadly expressed across CD8$^+$ T cell clusters irrespective of PT-Cy treatment (fig. S3) (*19*, *37*). When administered from 3 days after PT-Cy, both agonist immunotherapies promoted anti-myeloma responses, as evidenced by decreased M-bands at 4 and 6 weeks compared with PT-Cy alone (Fig. 6D). Although GVHD clinical scores were minimally elevated in agonist-treated mice, they remained below those of alloBMT recipients without PT-Cy (Fig. 6D), consistent with the absence of substantial GVHD.

We next investigated the mechanisms of action of DR-18 and anti-CD137 after PT-Cy. We observed a significant increase in the concentration of serum IFN-γ and, to a lesser extent, TNF in DR-18– but not anti-CD137–treated recipients compared with PT-Cy alone (Fig. 6E). We then tracked immune responses in individual mice over time using serial BM aspirates. At 4 weeks after alloBMT, CD8$^+$ T cells from PT-Cy–treated mice could be grouped into three populations: nonactivated/bystander (DNAM-1$^+$TIGIT$^-$ and CD39$^-$TIM3$^-$), activated/effector (DNAM-1$^+$TIGIT$^+$ and CD39^{int}TIM3$^-$), and exhausted (DNAM-1$^-$TIGIT$^+$ and CD39^{hi}TIM3$^+$) cells. DR-18 preferentially expanded the activated/effector T cell subset, whereas anti-CD137 promoted the exhausted phenotype (Fig. 6F), an outcome possibly driven by the stem-like properties of the CD8$^+$ T cells expressing IL-18R. Natural killer (NK) cells were also expanded in DR-18–treated mice (Fig. 6G). There was an almost complete elimination of MM cells from the BM of recipients treated with DR-18 or anti-CD137 by 6 weeks after alloBMT (Fig. 6H). At this 6-week time point, we also noted an expansion of CD8$^+$ and CD4$^+$ T cells in anti-CD137–treated mice in BM but not in blood (Fig. 6I and fig. S11A). In DR-18–treated mice, there was no change in T cell numbers; however, the number of DNAM-1$^+$ and cytolytic NK cells was significantly increased specifically in the marrow but not in the blood (Fig. 6, I and J, and fig. S11, A and B).

Unbiased clustering of CD4$^+$ and CD8$^+$ T cell flow cytometry data using FlowSOM revealed differential relative expansion of several immune phenotypes across treatment groups (Fig. 6, K and L) (*38*). Heatmaps depict mean fluorescence intensity (MFI) of each included marker across 12 populations within CD4$^+$ T cells (fig. S12A). In αCD137-treated mice, regulatory T (T_{reg}) frequency was reduced, whereas exhausted and effector CD4$^+$ T cell subsets were increased compared with DR-18–treated and PT-Cy–only recipients (fig. S12B). DR-18 treatment specifically expanded a CD62L$^-$ T_{reg} population (fig. S12C), suggested to be less suppressive and highly activated (*39*), without expanding the overall frequency of T_{regs} compared with PT-Cy–only recipients. In the CD8$^+$ T cell compartment, DR-18 promoted CD8$^+$ T cell activation with a relative enrichment in nonexhausted effector populations (Fig. 6L and fig. S13) and increased frequency of DNAM-1$^+$TIGIT$^+$ and CD39^{int}TIM3$^-$ subsets (Fig. 6, M and N) compared with PT-Cy alone recipients. At this time point, CD8$^+$ T cells from αCD137-treated recipients were largely terminally exhausted (Fig. 6, L to N), although the total number of cytotoxic granzyme B$^+$ or perforin$^+$ CD8$^+$ T cells was increased (Fig. 6, O and P). In the blood, DR-18 reduced the total number of CD4$^+$ and CD8$^+$ T cells; however, treatment increased the frequency of T_{EM} in both compartments (fig. S11, A, C, and D). Treatment with αCD137 increased expression of granzyme B, PD-1, CD39, and TOX on CD8$^+$ T cells in the blood but not to the same extent as observed in the BM (fig. S11E). Therefore, agonist immunotherapy promoted immune cell activation, largely in the BM TME, and generated potent myeloma immunity after PT-Cy. DR-18 treatment generated a less terminally exhausted phenotype compared with anti-CD137, potentially due to the expression of IL-18R on stem-like CD8$^+$ and CD4$^+$ T cells after PT-Cy.

Decoy-resistant IL-18 promotes potent GVL effects

We next sought to explore the combination of agonist immunotherapy with PT-Cy in a model of haploidentical transplantation (haploBMT), a setting where PT-Cy is a clinical standard of care. In this model, there is a major genetic mismatch between the recipient and the donor whereby lethal GVHD occurs in the absence of any immunosuppressive interventions. Here, we used a BCR-ABL-NUP98-HOXA9 leukemia, which is GVL-sensitive (Fig. 7A). In this model, untreated haploBMT recipients developed lethal GVHD, and although PT-Cy reduced the incidence of lethal GVHD, treatment increased relapse-related mortality such that there was no difference in overall survival (Fig. 7B). DR-18 administration after PT-Cy significantly improved GVL responses and overall survival, whereas CD137 agonism had no antitumor efficacy in this model (Fig. 7B).

To explore the mechanisms of DR-18–driven GVL in a haploBMT setting, we used donor cells from a triple reporter mouse (FoxP3-RFP × IL-10–GFP × IFN-γ–YFP) to measure in vivo cytokine production without restimulation. We performed phenotyping in mice with low leukemia burden to minimize the effect of tumor cells on T cell number in the BM. PT-Cy–treated recipients had reduced CD8$^+$ T cell numbers in the BM but increased NK cells compared with untreated haploBMT recipients (Fig. 7C). The frequency of IFN-γ$^+$ CD8$^+$ T cells was minimally decreased after PT-Cy, whereas CD4$^+$ IFN-γ production was unaffected (Fig. 7D). DR-18 did not alter IFN-γ production from T cells after PT-Cy (Fig. 7D) but did increase DNAM-1 expression (Fig. 7, E and F) and reduced TOX and TIM-3 expression (Fig. 7G) on CD8$^+$ T cells. CD8$^+$ T cells from DR-18–treated recipients also had significantly increased granzyme B (GrzB) and granzyme A (GrzA) secretion compared with both untreated haploBMT recipients and PT-Cy alone (Fig. 7H). DR-18 also increased the frequency of IFN-γ–producing and GrzA$^+$GrzB$^+$ NK cells compared with both PT-Cy alone and untreated haploBMT recipients (Fig. 7, I and J). Together, these data highlight the ability of DR-18 to drive potent GVL effects by reducing CD8$^+$ T cell exhaustion and expanding cytotoxic NK cells after haploBMT with PT-Cy.

DISCUSSION

Allogeneic BMT is the only curative treatment for many hematological malignancies; however, some malignancies, particularly myeloma, are inherently resistant to GVT effects. Here, we developed murine models of alloBMT that recapitulate these clinical observations to uncover the immunological mechanisms therein. High expression of inhibitory receptors after alloBMT in the absence of tumor antigen, together with our observed lack of GVM but

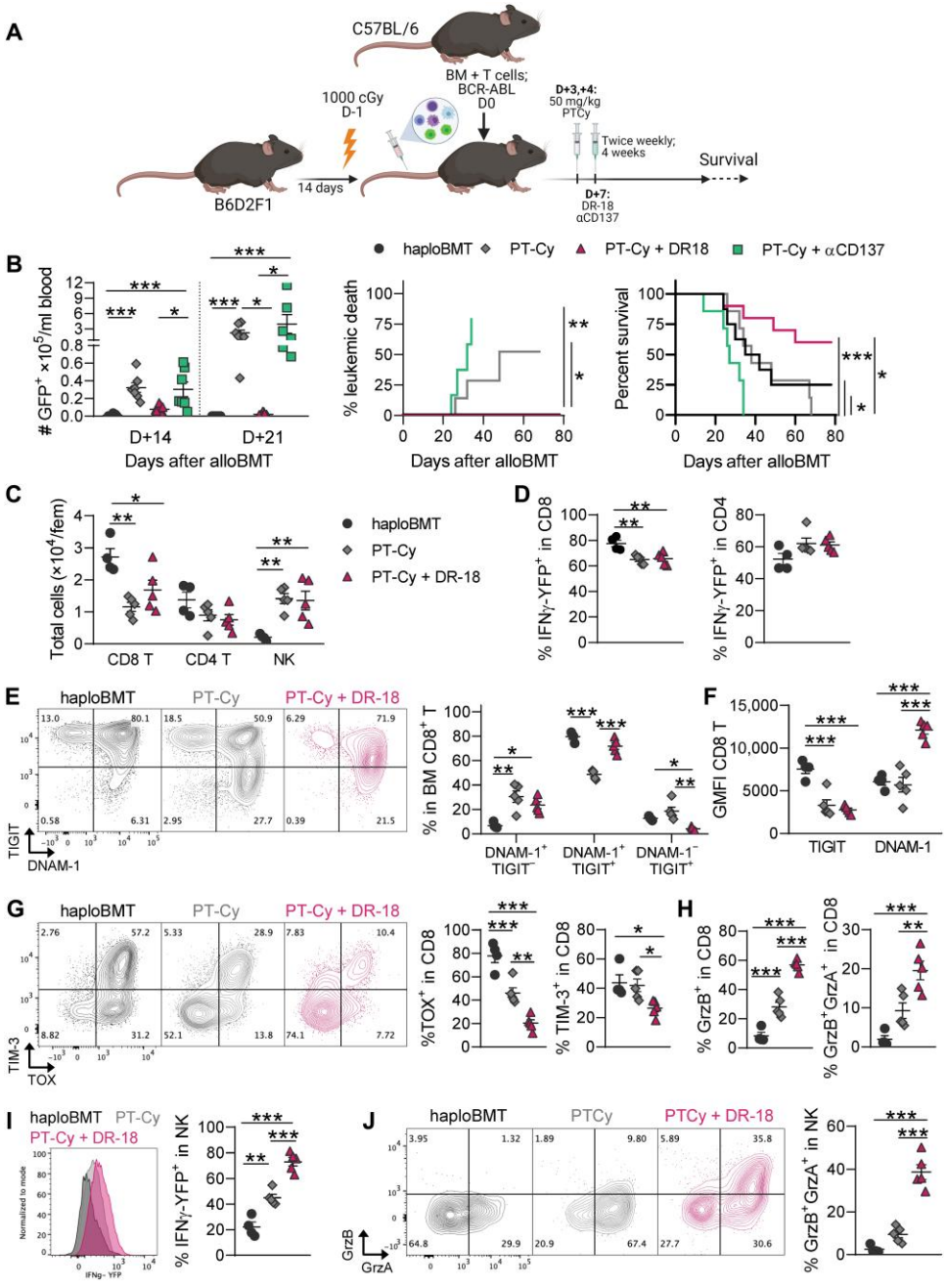

Fig. 7. DR-18 promotes GVL after haploidentical transplantation. B6D2F1 recipients were lethally irradiated and transplanted with 5×10^6 BM and 2×10^6 T cells from HULK (IFN-γ–YFP × IL-10–GFP × FoxP3-RFP) donors and 1×10^6 BCR-ABL-NUP98-HOXA9 leukemia cells. Recipients were untreated (haploBMT) or administered PT-Cy (50 mg/kg) on D+3 and D+4 (PT-Cy) with or without decoy-resistant IL-18 (PT-Cy + DR-18; 8 μg twice weekly from D+7 to week 5) or CD137 agonist antibody (PT-Cy + αCD137; 100 μg twice weekly from D+7 to week 5). (**A**) Experimental design. (**B**) Number of GFP^+ leukemia cells in blood, leukemic death, and overall median survival. (**C** to **J**) Mice with <5% leukemia cells in BM were euthanized at 21 days after transplantation, and BM was analyzed ($n = 4$ to 5; one experiment). (C) Total numbers of $CD8^+$ T, $CD4^+$ T, and NK cells. (D) Percentage of IFN-γ–producing $CD8^+$ and $CD4^+$ T cells. (E) Coexpression of DNAM-1 and TIGIT and (F) MFI on $CD8^+$ T cells. (G) Expression of TIM-3 and TOX on $CD8^+$ T cells. (H) Granzyme A and B expression in $CD8^+$ T cells. (I) IFN-γ and (J) granzyme A and B production in NK cells. One-way ANOVA with Tukey's multiple comparisons test and log-rank for survival. Data are means ± SEM. *$P < 0.05$, **$P < 0.01$, and ***$P < 0.001$.

exacerbated GVHD after ICI, suggests that alloantigen primarily drives T cell exhaustion after alloBMT in myeloma. Up-regulation of TIGIT and PD-1 on $CD8^+$ T cells after alloBMT presumably enhanced myeloma-mediated suppression of activated alloreactive T cells in a tumor antigen–independent manner, because both PD-L1 and CD155 were highly expressed on VK12653 but were largely absent on MLL-AF9–driven AML. The reduction in IFN-γ production in $CD8^+$ T cells from mice with relapsed AML compared with AML-free mice suggests that these T cells were at a more terminal stage of dysfunction that was driven by tumor antigen. Nonetheless, a previous study has shown that TIGIT inhibition did not enhance GVL in a preclinical AML model, although anti–PD-1 did provide some antitumor activity (*40*). Vk*MYC myeloma expresses clinically relevant inhibitory ligands: Both CD155 and PD-L1 have been observed on malignant plasma cells in patients with myeloma (*41*–*46*). Furthermore, these ligands are expressed on AML cells in some patients and may also contribute to GVT resistance and/or immune escape across several hematological malignancies (*47*–*49*).

The interaction of inhibitory ligands with their coupled receptors on T cells inhibits T cell cytolytic activity, reduces effector cytokine production, limits proliferation, and results in T cell apoptosis (*50*, *51*). Inhibitory receptors are also highly expressed on human $CD8^+$ T cells in patients receiving either matched or haploidentical donor grafts (*52*, *53*). Patients with relapsed disease after matched alloBMT had increased expression of inhibitory receptors on BM $CD8^+$ T cells compared with those achieving a complete response (*52*, *54*), whereas there was no effect of tumor relapse on T cell exhaustion in haploidentical alloBMT recipients (*52*). These clinical observations corroborate our hypothesis that alloantigen is a key driver of T cell exhaustion after alloBMT. These effects make subtle changes in T cell exhaustion at relapse difficult to ascertain, and examination of this will require longitudinal analysis of $CD8^+$ T cell subsets by single-cell approaches in large prospective studies of PT-Cy versus standard immunosuppression in patients who relapse versus those who do not. Together with our findings, these data suggest that subversion of alloreactive T cells by inhibitory ligand expression may be operative in hematological malignancies.

Alloantigen increased the expression not only of inhibitory receptors by donor T cells but also of exhaustion-associated gene signatures, chromatin accessibility within exhaustion-associated genes, and exhaustion-associated motifs. PT-Cy reduced these exhaustion signatures in both $CD8^+$ and $CD4^+$ T cells and instead enriched for stem-like memory phenotypes and *Tcf7*-driven motifs. We propose that establishment of a myeloma-driven exhaustion phenotype at relapse enabled agonistic immunotherapy interventions capable of enhancing myeloma-specific immunity without driving the lethal GVHD (as seen after ICI in the absence of PT-Cy). The inability of ICI to drive myeloma immunity after PT-Cy is likely due to cytoreduction of T cells and/or the absence of inhibitory receptor expression on T_{SCM} cells that are specifically enriched after PT-Cy. T_{SCM} cells have been described in the peripheral blood of patients after PT-Cy, and our data demonstrate that T_{SCM} reside in the BM and have high expression of the IL-18R (*55*, *56*). Furthermore, we have demonstrated that human T_{SCM} express the IL-18R after alloBMT. DR-18 administration after PT-Cy may act directly on these T_{SCM} cells to promote myeloma immunity and IFN-γ production. IFN-γ secretion by donor $CD8^+$ T cells is inversely correlated with their ability to cause GVHD, explaining the absence of lethal GVHD after DR-18 (*57*). The lack of ICI efficacy and the potent antitumor effects of DR-18 also reflect the need for agonists that act as an accelerator to drive T cell activation after PT-Cy rather than the need for antibodies that block immunological brakes, checkpoints, in cells that are putatively not highly activated at the time of immunotherapy.

The mechanisms of action of PT-Cy have been explored in other studies using very high donor T cell doses and variable but often lower cyclophosphamide doses than used in our studies and clinically (*58*, *59*). These studies demonstrate donor T cell depletion with relative sparing of regulatory T cells. Whether alloreactive T cells are differentially depleted by PT-Cy is less clear, with disparate results depending on the T cell dose and alloreactive T cell clone being tracked. Certainly, we have noted early and profound depletion of all donor T cells, including alloreactive clones, by PT-Cy. Likewise, the effect of PT-Cy on GVL, if any, is not clear in clinical studies where patients are transplanted with heterogeneous malignancies and levels of measurable residual disease that limit the power to discriminate effects (*60*–*63*). The number of T cells needed to mediate an effective GVL response is substantially lower than that required to mediate lethal GVHD, and so, T cell depletion in vivo by PT-Cy does not necessarily mitigate an effective GVL, although it is likely quantitatively modified. A recent study provides clinical support for our hypothesis that PT-Cy reduces alloantigen T cell exhaustion and instead facilitates tumor-driven T cell exhaustion. In this study, the authors observed a broad reduction in T cell exhaustion signatures by gene set enrichment analysis in patients treated with PT-Cy, which was then increased in patients who went on to relapse (*64*). In our study, we demonstrated that T cell exhaustion only occurred in the presence of high myeloma burden in the BM after PT-Cy, despite the fact that alloantigen persists at this site indefinitely through residual recipient stromal cells (*65*). Together, these data strongly suggest that tumor antigen, rather than alloantigen, drives T cell exhaustion after PT-Cy; however, this hypothesis requires formal examination in subsequent studies.

Utilization of donor NK cells to enhance GVL is being increasingly studied, particularly in the context of haploidentical transplantation where missing MHC class I and NK-sensitive AML represent favorable immunological contexts to exploit this effect (*66*, *67*). This is particularly relevant for DR-18, because this cytokine had a stimulatory effect on NK cells, in addition to the effects on $CD8^+$ T cells in both our transplantation models and previously published solid tumor systems (*35*). We have not excluded this effect as a complementary mechanism of antitumor activity, and it is highly likely that the combination of both T and NK cell–mediated GVL is operative. AML is particularly sensitive to NK cell–mediated killing, and this may underlie the lack of efficacy of CD137 agonism in leukemia, because αCD137 did not elicit the same NK cell expansion and activation as was seen with DR-18.

In conclusion, we have identified a previously unappreciated mechanism of ineffective GVT after alloBMT whereby T cell exhaustion is driven primarily by alloantigen and exacerbation of GVHD does not confer enhanced GVM. Rather, the use of PT-Cy eliminated donor T cell exhaustion signatures and enriched for stem cell memory gene activity early post-alloBMT. This immunophenotype can be targeted with agonistic immunotherapy approaches to enhance GVM and GVL without exacerbating GVHD in both MHC-matched and haploidentical transplantation models. These

data provide the rationale for investigation of the use of PT-Cy–based immunosuppression as a platform for subsequent agonist immunotherapies after allogenic stem cell transplantation. More broadly, our data demonstrate that stem-like memory T cells are more responsive to agonist immunotherapies than ICI and can be targeted by DR-18 to promote antitumor effects without driving terminal T cell exhaustion.

MATERIALS AND METHODS

Study design

This study was designed to interrogate mechanisms behind ineffective GVT responses after allogeneic stem cell transplantation. We developed murine models that were sensitive or resistant to GVT effects and used flow cytometry alongside multiomic single-cell RNA sequencing approaches to interrogate CD4 and CD8 T cell phenotypes in the BM. We then used PT-Cy and agonist immunotherapies to overcome GVT resistance and drive potent antitumor responses. Mice were randomly assigned to groups in all experiments without investigator blinding. All *n* values reflect biological replicates, and numbers of mice per group are included, with the statistical test performed, in the caption for each figure.

Mice

Female C57Bl/6 mice were purchased from the Animal Resources Centre (Perth, Western Australia, AUS) or the Jackson Laboratory (Bar Harbor, ME, USA). C3H.SW mice were purchased from the Jackson Laboratory and subsequently bred in house (QIMR Berghofer Medical Research Institute, Brisbane, QLD, Australia; Fred Hutchinson Cancer Center, Seattle, WA, USA). Female B6D2F1 mice were purchased from Charles River and subsequently bred in house (Fred Hutchinson Cancer Center). FoxP3-RFP × IL-10–GFP × IFN-γ–YFP mice were bred in house (Fred Hutchinson Cancer Center). Mice were housed in sterile microisolator cages and received acidified (pH 2.5), autoclaved water and normal chow. Mice were 8 to 12 weeks of age when used in experiments. All animal procedures were performed in accordance with protocols approved by the institutional animal ethics committee.

Stem cell transplantation

Recipient mice were intravenously injected with Vk12653, which originated from Vk*MYC transgenic mice (*68*, *69*), 2 weeks before BMT (1×10^6 $CD138^+CD19^{neg}$ cells; MM-bearing mice) or with an MLL-AF9–driven AML (MLL-AF9; 0.1×10^6 GFP^+) or BCR-ABL-NUP98-HOXA9 (1.0×10^6 GFP^+) on D0 (AML-bearing mice) (*70*, *71*). Recipients were transplanted as described previously with BM and T cell grafts (doses detailed in the figure legends) administered via tail vein injection the day after lethal irradiation (1000 cGy for C57Bl/6 and 1100 cGy for B62DF1, ^{137}Cs source) (*72*). Every 2 weeks, serum samples were collected from MM-bearing recipients, and M-band was quantified as previously described using a Sebia Hydrasys serum protein electrophoresis system (HYDRASYS 2 Scan) (*68*). Leukemia cell number in blood was calculated weekly using flow cytometry to quantify GFP^+ cells in blood. Recipients were monitored daily, up to 120 days after BMT, and euthanized when hindlimb paralysis occurred or clinical scores reached ≥6 (*73*). In competing risk analyses, deaths were attributed to myeloma if the M-band was above 0.28, a previously defined relapse threshold (*19*). In the leukemia models, leukemic death was defined by a white blood cell count above 50×10^6/ml or a GFP^+ leukemia frequency above 50% in blood or BM.

For some experiments, mice were treated with 100 μg of anti-TIGIT monoclonal antibody (mAb; 4B1, Bristol Myers Squibb) or mouse IgG2a (anti-KLH) twice a week for 4 weeks from D+14 post-alloBMT. For other experiments, mice were treated with 100 μg of Fc-dead anti-TIGIT mAb (D265A, Bristol Myers Squibb) or mouse IgG1 (anti-KLH.1) twice a week for 6 weeks from D+21 post-alloBMT. Cyclophosphamide (Fisher Scientific; 99.5%, MP Biomedicals) was intraperitoneally administered at 50 mg/kg on D+3 and D+4 after alloBMT (PT-Cy). After PT-Cy, 100 μg of anti–TIM-3 mAb (RMT3-23, Bio X Cell), anti–PD-1 mAb (RMP1-14, Bio X Cell), or anti-CD137 (4-1BB, 3H3, Bio X Cell) and related isotypes were intraperitoneally administered twice a week, whereas 8 μg of DR-18 [described (*35*)] was subcutaneously administered twice a week from D+7 for 4 weeks. DR-18 was supplied by Simcha Therapeutics (New Haven, CT).

Cell preparation for flow cytometry

Recipient mice were euthanized 2 to 8 weeks after transplant, and cells from BM or blood were harvested. For BM aspirates, mice were anesthetized and treated with a local analgesic (0.5% lidocaine) followed by injection of 30 μl of phosphate-buffered saline (PBS) into the femur to allow up to 10 μl of marrow to be aspirated for fluorescence-activated cell sorting (FACS) analysis. For surface marker phenotyping, isolated cells were incubated with Fc-block before staining with fluorescently tagged antibodies (listed in table S1), on ice for 30 min. For intracellular staining, cells were surface-labeled, fixed, and permeabilized (eBioscience, Foxp3 Transcription Factor Staining Buffer Kit) before intracellular staining at room temperature for 60 min. To measure cytokine production, we stimulated cells for 4 hours at 37°C with PMA (500 ng/ml) and ionomycin (50 ng/ml; Sigma-Aldrich) with brefeldin A (BioLegend). All samples were acquired on a BD LSR Fortessa (BD Biosciences) or BD FACSymphony A3 (BD Biosciences) and analyzed using FlowJo software (v10). t-SNE analysis was performed using the FlowJo plugin with default settings on a concatenated sample with 3000 CD8 T cells per mouse. FlowSOM analysis was performed with 3000 to 4000 CD8 or CD4 T cells per mouse concatenated after downsampling (*38*).

Single-cell RNA/ATAC sequencing

Naïve C57Bl/6 mice were transplanted with C3H.SW grafts and were untreated (alloBMT) or treated with PT-Cy (50 mg/kg) on D+3 and D+4 (PT-Cy). BM was harvested from femurs (four mice pooled per group) at D+14 after alloBMT, and T cells were sort-purified ($CD90.2^+CD4^+$ and $CD90.2^+CD8^+$) before nuclei preparation according to the 10x Genomics Multiome protocol (CG000365_DemonstratedProtocol_NucleiIsolation_ATAC_-GEX_Sequencing_RevB.pdf). Nuclei (also here referred to as cells) were captured and libraries were generated according to the manufacturer's specifications. Libraries were sequenced using Illumina NovaSeq 6000 targeting a depth of 25,000 reads per cell per library.

Single-cell RNA/ATAC analysis

Reads were demultiplexed and processed using cellranger-arc v1.0.1 aligning reads to GENCODE vM23/Ensembl98. Peaks were called from each sample's fragment file (cellranger output) using MACS2 (*74*) using the parameters "--nomodel --extsize 200

--shift -100." Quantification of reads in MACS2 peaks were calculated and integrated with cellranger RNA output using Signac (*75*). Cells meeting the following criteria (calculated using Signac) were retained for downstream analysis: percent mitochondrial RNA reads <10%; 3 > $\log_{10}$(ATAC counts) < 4.5; 3 > $\log_{10}$(RNA/UMI counts) < 4.5; fraction of reads in peaks >40%; transcription start site (TSS) percentile >75%. RNA/unique molecular identifier (UMI) counts were subject to a variance-stabilized normalization procedure using Seurat's (*76*) "glmGamPoi" (*77*) function before dimensionality reduction using principal components analysis (PCA). ATAC data after TFIDF/SVD (*75*) dimensionality reduction were integrated with reduced-dimensionality RNA data (PCA matrix) using the WNN (*78*) function with default parameters. CD4 and CD8 cells were defined using absolute RNA/UMI counts greater than 0. Cells with counts for both CD4 and CD8 were further excluded. Clusters were identified using the standard Seurat workflow. Gene activity scores and Motif scores were calculated using Signac (*75*) and chromVAR (*79*).

External data

To identify genes specific for T_{SCM} cells, we obtained publicly available single-cell RNA sequencing data from Gene Expression Omnibus (GSE152379) and processed using Seurat. To generate a high-confidence list of T_{SCM}-specific genes, we identified those genes specific to BACH2-overexpressing cells (*9*) using a strict filter of a q value of <0.001 and $\log_2$ fold change of >1, removing ribosomal protein genes (Rpl* and Rps*), and included critical T_{SCM} genes, Bach2, Bcl2, Eomes, Myb, and Tnfsf8. Gene set for exhaustion (Tex) was generated taking data from published bulk expression profiles (*29*) and filtered using the same cutoffs. Gene set scores were calculated using the AddModuleScore function in Seurat. Statistical test for gene set scores was calculated using Wilcoxon rank sum in R.

Human samples

Peripheral blood mononuclear cells from an Institutional Review Board–approved study of immune reconstitution in patients receiving allogeneic stem cell transplantation at the Fred Hutchinson Cancer Center were thawed and resuspended in prewarmed culture medium containing deoxyribonuclease (DNase) 1. Cells were washed twice with PBS before incubating with FVS440UV (BD Biosciences) and Fc Block (Human TruStain, BioLegend) for 15 min at room temperature. Cells were washed and then stained with surface flow cytometry antibodies for 30 min on ice. Cells were washed and fixed with eBioscience FoxP3 staining kit according to the manufacturer's protocol before intracellular staining at room temperature for 1 hour.

Statistical analysis

Data are presented as means ± SEM, and $P < 0.05$ was considered significant. Survival curves were plotted using Kaplan-Meier estimates and compared by log-rank (Mantel-Cox) test. M-bands were modeled as previously described (*3*, *19*), and the M-band relapse threshold (G/A above 0.282) has been previously reported (*3*, *19*). Competing risk analysis was performed using the cmprsk R package. Comparisons between two groups were performed with t test or Mann-Whitney U test, and comparisons between three or more groups were performed with one-way analysis of variance (ANOVA) and Tukey's multiple comparisons test for normally distributed data or with Kruskal-Wallis and Dunn's multiple comparisons test for nonparametric data.

Supplementary Materials

This PDF file includes:
Figs. S1 to S13
Table S1

Other Supplementary Material for this manuscript includes the following:
Data files S1 to S3
MDAR Reproducibility Checklist

View/request a protocol for this paper from *Bio-protocol*.

REFERENCES AND NOTES

1. C. U. Blank, W. N. Haining, W. Held, P. G. Hogan, A. Kallies, E. Lugli, R. C. Lynn, M. Philip, A. Rao, N. P. Restifo, A. Schietinger, T. N. Schumacher, P. L. Schwartzberg, A. H. Sharpe, D. E. Speiser, E. J. Wherry, B. A. Youngblood, D. Zehn, Defining 'T cell exhaustion'. *Nat. Rev. Immunol.* **19**, 665–674 (2019).
2. D. J. Chung, K. B. Pronschinske, J. A. Shyer, S. Sharma, S. Leung, S. A. Curran, A. M. Lesokhin, S. M. Devlin, S. A. Giralt, J. W. Young, T-cell exhaustion in multiple myeloma relapse after autotransplant: Optimal timing of immunotherapy. *Cancer Immunol. Res.* **4**, 61–71 (2016).
3. S. A. Minnie, R. D. Kuns, K. H. Gartlan, P. Zhang, A. N. Wilkinson, L. Samson, C. Guillerey, C. Engwerda, K. P. A. MacDonald, M. J. Smyth, K. A. Markey, S. Vuckovic, G. R. Hill, Myeloma escape after stem cell transplantation is a consequence of T-cell exhaustion and is prevented by TIGIT blockade. *Blood* **132**, 1675–1688 (2018).
4. C. Zelle-Rieser, S. Thangavadivel, R. Biedermann, A. Brunner, P. Stoitzner, E. Willenbacher, R. Greil, K. Johrer, T cells in multiple myeloma display features of exhaustion and senescence at the tumor site. *J. Hematol. Oncol.* **9**, 116 (2016).
5. A. Haslam, V. Prasad, Estimation of the percentage of US patients with cancer who are eligible for and respond to checkpoint inhibitor immunotherapy drugs. *JAMA Netw. Open* **2**, e192535 (2019).
6. P. Armand, A. Engert, A. Younes, M. Fanale, A. Santoro, P. L. Zinzani, J. M. Timmerman, G. P. Collins, R. Ramchandren, J. B. Cohen, J. P. De Boer, J. Kuruvilla, K. J. Savage, M. Trneny, M. A. Shipp, K. Kato, A. Sumbul, B. Farsaci, S. M. Ansell, Nivolumab for relapsed/refractory classic hodgkin lymphoma after failure of autologous hematopoietic cell transplantation: Extended follow-up of the multicohort single-arm phase II checkmate 205 trial. *J. Clin. Oncol.* **36**, 1428–1439 (2018).
7. R. Ramchandren, E. Domingo-Domènech, A. Rueda, M. Trněný, T. A. Feldman, H. J. Lee, M. Provencio, C. Sillaber, J. B. Cohen, K. J. Savage, W. Willenbacher, A. H. Ligon, J. Ouyang, R. Redd, S. J. Rodig, M. A. Shipp, M. Sacchi, A. Sumbul, P. Armand, S. M. Ansell, Nivolumab for newly diagnosed advanced-stage classic hodgkin lymphoma: Safety and efficacy in the phase II checkmate 205 study. *J. Clin. Oncol.* **37**, 1997–2007 (2019).
8. I. Siddiqui, K. Schaeuble, V. Chennupati, S. A. Fuertes Marraco, S. Calderon-Copete, D. Pais Ferreira, S. J. Carmona, L. Scarpellino, D. Gfeller, S. Pradervand, S. A. Luther, D. E. Speiser, W. Held, Intratumoral Tcf1$^+$PD-1$^+$CD8$^+$ t cells with stem-like properties promote tumor control in response to vaccination and checkpoint blockade immunotherapy. *Immunity* **50**, 195–211.e10 (2019).
9. C. Yao, G. Lou, H. W. Sun, Z. Zhu, Y. Sun, Z. Chen, D. Chauss, E. A. Moseman, J. Cheng, M. A. D'Antonio, W. Shi, J. Shi, K. Kometani, T. Kurosaki, E. J. Wherry, B. Afzali, L. Gattinoni, Y. Zhu, D. B. McGavern, J. J. O'Shea, P. L. Schwartzberg, T. Wu, BACH2 enforces the transcriptional and epigenetic programs of stem-like CD8$^+$ T cells. *Nat. Immunol.* **22**, 370–380 (2021).
10. J. A. Fraietta, S. F. Lacey, E. J. Orlando, I. Pruteanu-Malinici, M. Gohil, S. Lundh, A. C. Boesteanu, Y. Wang, R. S. O'Connor, W. T. Hwang, E. Pequignot, D. E. Ambrose, C. Zhang, N. Wilcox, F. Bedoya, C. Dorfmeier, F. Chen, L. Tian, H. Parakandi, M. Gupta, R. M. Young, F. B. Johnson, I. Kulikovskaya, L. Liu, J. Xu, S. H. Kassim, M. M. Davis, B. L. Levine, N. V. Frey, D. L. Siegel, A. C. Huang, E. J. Wherry, H. Bitter, J. L. Brogdon, D. L. Porter, C. H. June, J. J. Melenhorst, Determinants of response and resistance to CD19 chimeric antigen receptor (CAR) T cell therapy of chronic lymphocytic leukemia. *Nat. Med.* **24**, 563–571 (2018).
11. J. Aschan, B. Lönnqvist, O. Ringdén, G. Kumlien, G. Gahrton, Graft-versus-myeloma effect. *Lancet* **348**, 346 (1996).
12. G. Tricot, D. H. Vesole, S. Jagannath, J. Hilton, N. Munshi, B. Barlogie, Graft-versus-myeloma effect: Proof of principle. *Blood* **87**, 1196–1198 (1996).

13. W. I. Bensinger, Role of autologous and allogeneic stem cell transplantation in myeloma. *Leukemia* **23**, 442–448 (2009).
14. A. Ijaz, A. Y. Khan, S. U. Malik, W. Faridi, M. A. Fraz, M. Usman, M. J. Tariq, S. Durer, C. Durer, A. Russ, N. N. C. Parr, Z. Baig, F. N. U. Sagar, Z. Ali, A. McBride, F. Anwer, Significant risk of graft-versus-host disease with exposure to checkpoint inhibitors before and after allogeneic transplantation. *Biol. Blood Marrow Transplant.* **25**, 94–99 (2019).
15. B. M. Haverkos, D. Abbott, M. Hamadani, P. Armand, M. E. Flowers, R. Merryman, M. Kamdar, A. S. Kanate, A. Saad, A. Mehta, S. Ganguly, T. S. Fenske, P. Hari, R. Lowsky, L. Andritsos, M. Jagasia, A. Bashey, S. Brown, V. Bachanova, D. Stephens, S. Mineishi, R. Nakamura, Y.-B. Chen, B. R. Blazar, J. Gutman, S. M. Devine, PD-1 blockade for relapsed lymphoma post–allogeneic hematopoietic cell transplant: High response rate but frequent GVHD. *Blood* **130**, 221–228 (2017).
16. P. E. Rovatti, V. Gambacorta, F. Lorentino, F. Ciceri, L. Vago, Mechanisms of leukemia immune evasion and their role in relapse after haploidentical hematopoietic cell transplantation. *Front. Immunol.* **11**, 147 (2020).
17. X. Yin, L. Tang, F. Fan, Q. Jiang, C. Sun, Y. Hu, Allogeneic stem-cell transplantation for multiple myeloma: A systematic review and meta-analysis from 2007 to 2017. *Cancer Cell Int.* **18**, 62 (2018).
18. M. Stern, L. C. de Wreede, R. Brand, A. van Biezen, P. Dreger, M. Mohty, T. M. de Witte, N. Kröger, T. Ruutu, Sensitivity of hematological malignancies to graft-versus-host effects: An EBMT megafile analysis. *Leukemia* **28**, 2235–2240 (2014).
19. S. Vuckovic, S. A. Minnie, D. Smith, K. H. Gartlan, T. S. Watkins, K. A. Markey, P. Mukhopadhyay, C. Guillerey, R. D. Kuns, K. R. Locke, A. L. Pritchard, P. A. Johansson, A. Varelias, P. Zhang, N. D. Huntington, N. Waddell, M. Chesi, J. J. Miles, M. J. Smyth, G. R. Hill, Bone marrow transplantation generates T cell-dependent control of myeloma in mice. *J. Clin. Invest.* **129**, 106–121 (2019).
20. T. Inozume, K. Hanada, Q. J. Wang, M. Ahmadzadeh, J. R. Wunderlich, S. A. Rosenberg, J. C. Yang, Selection of $CD8^+PD\text{-}1^+$ lymphocytes in fresh human melanomas enriches for tumor-reactive T cells. *J. Immunother.* **33**, 956–964 (2010).
21. M. Braun, A. R. Aguilera, A. Sundarrajan, D. Corvino, K. Stannard, S. Krumeich, I. Das, L. G. Lima, L. G. M. Guzman, K. Li, R. Li, N. Salim, M. V. Jorge, S. Ham, G. Kelly, F. Vari, A. Lepletier, A. Raghavendra, S. Pearson, J. Madore, S. Jacquelin, M. Effern, B. Quine, L. T. Koufariotis, M. Casey, K. Nakamura, E. Y. Seo, M. Hölzel, M. Geyer, G. Kristiansen, T. Taheri, E. Ahern, B. G. M. Hughes, J. S. Wilmott, G. V. Long, R. A. Scolyer, M. D. Batstone, J. Landsberg, D. Dietrich, O. T. Pop, L. Flatz, W. C. Dougall, A. Veillette, S. E. Nicholson, A. Möller, R. J. Johnston, L. Martinet, M. J. Smyth, T. Bald, CD155 on tumor cells drives resistance to immunotherapy by inducing the degradation of the activating receptor CD226 in $CD8^+$ T cells. *Immunity* **53**, 805–823.e15 (2020).
22. X. Yu, K. Harden, L. C. Gonzalez, M. Francesco, E. Chiang, B. Irving, I. Tom, S. Ivelja, C. J. Refino, H. Clark, D. Eaton, J. L. Grogan, The surface protein TIGIT suppresses T cell activation by promoting the generation of mature immunoregulatory dendritic cells. *Nat. Immunol.* **10**, 48–57 (2009).
23. C. Herbaux, J. Gauthier, P. Brice, E. Drumez, L. Ysebaert, H. Doyen, L. Fornecker, K. Bouabdallah, G. Manson, H. Ghesquières, R. Tabrizi, E. Hermet, J. Lazarovici, A. Thiebaut-Bertrand, A. Chauchet, H. Demarquette, E. Boyle, R. Houot, I. Yakoub-Agha, F. Morschhauser, Efficacy and tolerability of nivolumab after allogeneic transplantation for relapsed Hodgkin lymphoma. *Blood* **129**, 2471–2478 (2017).
24. B. R. Blazar, B. M. Carreno, A. Panoskaltsis-Mortari, L. Carter, Y. Iwai, H. Yagita, H. Nishimura, P. A. Taylor, Blockade of programmed death-1 engagement accelerates graft-versus-host disease lethality by an IFN-γ-dependent mechanism. *J. Immunol.* **171**, 1272–1277 (2003).
25. A. Saha, K. Aoyama, P. A. Taylor, B. H. Koehn, R. G. Veenstra, A. Panoskaltsis-Mortari, D. H. Munn, W. J. Murphy, M. Azuma, H. Yagita, B. T. Fife, M. H. Sayegh, N. Najafian, G. Socie, R. Ahmed, G. J. Freeman, A. H. Sharpe, B. R. Blazar, Host programmed death ligand 1 is dominant over programmed death ligand 2 expression in regulating graft-versus-host disease lethality. *Blood* **122**, 3062–3073 (2013).
26. L. Wu, L. Mao, J.-F. Liu, L. Chen, G.-T. Yu, L.-L. Yang, H. Wu, L.-L. Bu, A. B. Kulkarni, W.-F. Zhang, Z.-J. Sun, Blockade of TIGIT/CD155 signaling reverses T-cell exhaustion and enhances antitumor capability in head and neck squamous cell carcinoma. *Cancer Immunol. Res.* **7**, 1700–1713 (2019).
27. J. Preillon, J. Cuende, V. Rabolli, L. Garnero, M. Mercier, N. Wald, A. Pappalardo, S. Denies, D. Jamart, A. C. Michaux, R. Pirson, V. Pitard, M. Bagot, S. Prasad, E. Houthuys, M. Brouwer, R. Marillier, F. Lambolez, J. R. Marchante, F. Nyawouame, M. J. Carter, V. Baron-Bodo, A. Marie-Cardine, M. Cragg, J. Déchanet-Merville, G. Driessens, C. Hoofd, Restoration of T-cell effector function, depletion of tregs, and direct killing of tumor cells: The multiple mechanisms of action of a-TIGIT antagonist antibodies. *Mol. Cancer Ther.* **20**, 121–131 (2021).
28. M. Philip, L. Fairchild, L. Sun, E. L. Horste, S. Camara, M. Shakiba, A. C. Scott, A. Viale, P. Lauer, T. Merghoub, M. D. Hellmann, J. D. Wolchok, C. S. Leslie, A. Schietinger, Chromatin states define tumour-specific T cell dysfunction and reprogramming. *Nature* **545**, 452–456 (2017).
29. A. C. Scott, F. Dundar, P. Zumbo, S. S. Chandran, C. A. Klebanoff, M. Shakiba, P. Trivedi, L. Menocal, H. Appleby, S. Camara, D. Zamarin, T. Walther, A. Snyder, M. R. Femia, E. A. Comen, H. Y. Wen, M. D. Hellmann, N. Anandasabapathy, Y. Liu, N. K. Altorki, P. Lauer, O. Levy, M. S. Glickman, J. Kaye, D. Betel, M. Philip, A. Schietinger, TOX is a critical regulator of tumour-specific T cell differentiation. *Nature* **571**, 270–274 (2019).
30. X. Liu, Y. Wang, H. Lu, J. Li, X. Yan, M. Xiao, J. Hao, A. Alekseev, H. Khong, T. Chen, R. Huang, J. Wu, Q. Zhao, Q. Wu, S. Xu, X. Wang, W. Jin, S. Yu, Y. Wang, L. Wei, A. Wang, B. Zhong, L. Ni, X. Liu, R. Nurieva, L. Ye, Q. Tian, X. W. Bian, C. Dong, Genome-wide analysis identifies NR4A1 as a key mediator of T cell dysfunction. *Nature* **567**, 525–529 (2019).
31. G. J. Martinez, R. M. Pereira, T. Äijö, E. Y. Kim, F. Marangoni, M. E. Pipkin, S. Togher, V. Heissmeyer, Y. C. Zhang, S. Crotty, E. D. Lamperti, K. M. Ansel, T. R. Mempel, H. Lähdesmäki, P. G. Hogan, A. Rao, The transcription factor NFAT promotes exhaustion of activated $CD8^+$ T cells. *Immunity* **42**, 265–278 (2015).
32. D. Pais Ferreira, J. G. Silva, T. Wyss, S. A. Fuertes Marraco, L. Scarpellino, M. Charmoy, R. Maas, I. Siddiqui, L. Tang, J. A. Joyce, M. Delorenzi, S. A. Luther, D. E. Speiser, W. Held, Central memory $CD8^+$ T cells derive from stem-like Tcf7hi effector cells in the absence of cytotoxic differentiation. *Immunity* **53**, 985–1000.e11 (2020).
33. W. H. Hudson, J. Gensheimer, M. Hashimoto, A. Wieland, R. M. Valanparambil, P. Li, J.-X. Lin, B. T. Konieczny, S. J. Im, G. J. Freeman, W. J. Leonard, H. T. Kissick, R. Ahmed, Proliferating transitory T cells with an effector-like transcriptional signature emerge from $PD\text{-}1^+$ stem-like $CD8^+$ T cells during chronic infection. *Immunity* **51**, 1043–1058.e4 (2019).
34. A. C. Huang, M. A. Postow, R. J. Orlowski, R. Mick, B. Bengsch, S. Manne, W. Xu, S. Harmon, J. R. Giles, B. Wenz, M. Adamow, D. Kuk, K. S. Panageas, C. Carrera, P. Wong, F. Quagliarello, B. Wubbenhorst, K. D'Andrea, K. E. Pauken, R. S. Herati, R. P. Staupe, J. M. Schenkel, S. McGettigan, S. Kothari, S. M. George, R. H. Vonderheide, R. K. Amaravadi, G. C. Karakousis, L. M. Schuchter, X. Xu, K. L. Nathanson, J. D. Wolchok, T. C. Gangadhar, E. J. Wherry, T-cell invigoration to tumour burden ratio associated with anti-PD-1 response. *Nature* **545**, 60–65 (2017).
35. T. Zhou, W. Damsky, O.-E. Weizman, M. K. McGeary, K. P. Hartmann, C. E. Rosen, S. Fischer, R. Jackson, R. A. Flavell, J. Wang, M. F. Sanmamed, M. W. Bosenberg, A. M. Ring, IL-18BP is a secreted immune checkpoint and barrier to IL-18 immunotherapy. *Nature* **583**, 609–614 (2020).
36. M.-L. Clénet, F. Gagnon, A. C. Moratalla, E. C. Viel, N. Arbour, Peripheral human $CD4^+CD8^+$ T lymphocytes exhibit a memory phenotype and enhanced responses to IL-2, IL-7 and IL-15. *Sci. Rep.* **7**, –11612 (2017).
37. C. Guillerey, K. Nakamura, A. C. Pichler, D. Barkauskas, S. Krumeich, K. Stannard, K. Miles, H. Harjunpää, Y. Yu, M. Casey, A. I. Doban, M. Lazar, G. Hartel, D. Smith, S. Vuckovic, M. W. Teng, P. L. Bergsagel, M. Chesi, G. R. Hill, L. Martinet, M. J. Smyth, Chemotherapy followed by anti-CD137 mAb immunotherapy improves disease control in a mouse myeloma model. *JCI Insight* **5**, e125932 (2019).
38. S. Van Gassen, B. Callebaut, M. J. Van Helden, B. N. Lambrecht, P. Demeester, T. Dhaene, Y. Saeys, FlowSOM: Using self-organizing maps for visualization and interpretation of cytometry data. *Cytometry A* **87**, 636–645 (2015).
39. E. Cretney, A. Xin, W. Shi, M. Minnich, F. Masson, M. Miasari, G. T. Belz, G. K. Smyth, M. Busslinger, S. L. Nutt, A. Kallies, The transcription factors Blimp-1 and IRF4 jointly control the differentiation and function of effector regulatory T cells. *Nat. Immunol.* **12**, 304–311 (2011).
40. M. Zhou, F. Sacirbegovic, K. Zhao, S. Rosenberger, W. D. Shlomchik, T cell exhaustion and a failure in antigen presentation drive resistance to the graft-versus-leukemia effect. *Nat. Commun.* **11**, 4227 (2020).
41. C. Fionda, M. P. Abruzzese, A. Zingoni, F. Cecere, E. Vulpis, G. Peruzzi, A. Soriani, R. Molfetta, R. Paolini, M. R. Ricciardi, M. T. Petrucci, A. Santoni, M. Cippitelli, The IMiDs targets IKZF-1/3 and IRF4 as novel negative regulators of NK cell-activating ligands expression in multiple myeloma. *Oncotarget* **6**, 23609–23630 (2015).
42. Y. M. El-Sherbiny, J. L. Meade, T. D. Holmes, D. McGonagle, S. L. Mackie, A. W. Morgan, G. Cook, S. Feyler, S. J. Richards, F. E. Davies, G. J. Morgan, G. P. Cook, The requirement for DNAM-1, NKG2D, and NKp46 in the natural killer cell-mediated killing of myeloma cells. *Cancer Res.* **67**, 8444–8449 (2007).
43. S. Yousef, J. Marvin, M. Steinbach, A. Langemo, T. Kovacsovics, M. Binder, N. Kröger, T. Luetkens, D. Atanackovic, Immunomodulatory molecule PD-L1 is expressed on malignant plasma cells and myeloma-propagating pre-plasma cells in the bone marrow of multiple myeloma patients. *Blood Cancer J.* **5**, e285 (2015).
44. N. J. Bahlis, A. M. King, D. Kolonias, L. M. Carlson, H. Y. Liu, M. A. Hussein, H. R. Terebelo, G. E. Byrne Jr., B. L. Levine, L. H. Boise, K. P. Lee, CD28-mediated regulation of multiple myeloma cell proliferation and survival. *Blood* **109**, 5002–5010 (2007).
45. M. Ishibashi, H. Tamura, M. Sunakawa, A. Kondo-Onodera, N. Okuyama, Y. Hamada, K. Moriya, I. Choi, K. Tamada, K. Inokuchi, Myeloma drug resistance induced by binding of myeloma B7-H1 (PD-L1) to PD-1. *Cancer Immunol. Res.* **4**, 779–788 (2016).

46. L. Wang, H. Wang, H. Chen, W. D. Wang, X. Q. Chen, Q. R. Geng, Z. J. Xia, Y. Lu, Serum levels of soluble programmed death ligand 1 predict treatment response and progression free survival in multiple myeloma. *Oncotarget* **6**, 41228–41236 (2015).
47. M. G. M. Roemer, R. A. Redd, F. Z. Cader, C. J. Pak, S. Abdelrahman, J. Ouyang, S. Sasse, A. Younes, M. Fanale, A. Santoro, P. L. Zinzani, J. Timmerman, G. P. Collins, R. Ramchandren, J. B. Cohen, J. P. De Boer, J. Kuruvilla, K. J. Savage, M. Trneny, S. Ansell, K. Kato, B. Farsaci, A. Sumbul, P. Armand, D. S. Neuberg, G. S. Pinkus, A. H. Ligon, S. J. Rodig, M. A. Shipp, Major histocompatibility complex class II and programmed death ligand 1 expression predict outcome after programmed death 1 blockade in classic hodgkin lymphoma. *J. Clin. Oncol.* **36**, 942–950 (2018).
48. A. Prestipino, A. J. Emhardt, K. Aumann, D. O'Sullivan, S. P. Gorantla, S. Duquesne, W. Melchinger, L. Braun, S. Vuckovic, M. Boerries, H. Busch, S. Halbach, S. Pennisi, T. Poggio, P. Apostolova, P. Veratti, M. Hettich, G. Niedermann, M. Bartholomä, K. Shoumariyeh, J. S. Jutzi, J. Wehrle, C. Dierks, H. Becker, A. Schmitt-Graeff, M. Follo, D. Pfeifer, J. Rohr, S. Fuchs, S. Ehl, F. A. Hartl, S. Minguet, C. Miething, F. H. Heidel, N. Kröger, I. Triviai, T. Brummer, J. Finke, A. L. Illert, E. Ruggiero, C. Bonini, J. Duyster, H. L. Pahl, S. W. Lane, G. R. Hill, B. R. Blazar, N. von Bubnoff, E. L. Pearce, R. Zeiser, Oncogenic JAK2(V617F) causes PD-L1 expression, mediating immune escape in myeloproliferative neoplasms. *Sci. Transl. Med.* **10**, eaam7729 (2018).
49. W. J. Norde, F. Maas, W. Hobo, A. Korman, M. Quigley, M. G. Kester, K. Hebeda, J. H. Falkenburg, N. Schaap, T. M. de Witte, R. van der Voort, H. Dolstra, PD-1/PD-L1 interactions contribute to functional T-cell impairment in patients who relapse with cancer after allogeneic stem cell transplantation. *Cancer Res.* **71**, 5111–5122 (2011).
50. N. Joller, J. P. Hafler, B. Brynedal, N. Kassam, S. Spoerl, S. D. Levin, A. H. Sharpe, V. K. Kuchroo, Cutting edge: TIGIT has T cell-intrinsic inhibitory functions. *J. Immunol.* **186**, 1338–1342 (2011).
51. J. Rosenblatt, D. Avigan, Targeting the PD-1/PD-L1 axis in multiple myeloma: A dream or a reality? *Blood* **129**, 275–279 (2017).
52. M. Noviello, F. Manfredi, E. Ruggiero, T. Perini, G. Oliveira, F. Cortesi, P. De Simone, C. Toffalori, V. Gambacorta, R. Greco, J. Peccatori, M. Casucci, G. Casorati, P. Dellabona, M. Onozawa, T. Teshima, M. Griffioen, C. J. M. Halkes, J. H. F. Falkenburg, F. Stölzel, H. Altmann, M. Bornhäuser, M. Waterhouse, R. Zeiser, J. Finke, N. Cieri, A. Bondanza, L. Vago, F. Ciceri, C. Bonini, Bone marrow central memory and memory stem T-cell exhaustion in AML patients relapsing after HSCT. *Nat. Commun.* **10**, 1065 (2019).
53. F. Simonetta, A. Pradier, C. Bosshard, S. Masouridi-Levrat, C. Dantin, A. Koutsi, Y. Tirefort, E. Roosnek, Y. Chalandon, Dynamics of expression of programmed cell death protein-1 (PD-1) on T cells after allogeneic hematopoietic stem cell transplantation. *Front. Immunol.* **10**, 1034 (2019).
54. T. J. A. Hutten, W. J. Norde, R. Woestenenk, R. C. Wang, F. Maas, M. Kester, J. H. F. Falkenburg, S. Berglund, L. Luznik, J. H. Jansen, N. Schaap, H. Dolstra, W. Hobo, Increased coexpression of PD-1, TIGIT, and KLRG-1 on tumor-reactive $CD8^+$ T cells during relapse after allogeneic stem cell transplantation. *Biol. Blood Marrow Transplant.* **24**, 666–677 (2018).
55. A. Roberto, L. Castagna, V. Zanon, S. Bramanti, R. Crocchiolo, J. E. McLaren, S. Gandolfi, P. Tentorio, B. Sarina, I. Timofeeva, A. Santoro, C. Carlo-Stella, B. Bruno, C. Carniti, P. Corradini, E. Gostick, K. Ladell, D. A. Price, M. Roederer, D. Mavilio, E. Lugli, Role of naive-derived T memory stem cells in T-cell reconstitution following allogeneic transplantation. *Blood* **125**, 2855–2864 (2015).
56. N. Cieri, B. Camisa, F. Cocchiarella, M. Forcato, G. Oliveira, E. Provasi, A. Bondanza, C. Bordignon, J. Peccatori, F. Ciceri, M. T. Lupo-Stanghellini, F. Mavilio, A. Mondino, S. Bicciato, A. Recchia, C. Bonini, IL-7 and IL-15 instruct the generation of human memory stem T cells from naive precursors. *Blood* **121**, 573–584 (2013).
57. Y.-G. Yang, J. Qi, M.-G. Wang, M. Sykes, Donor-derived interferon γ separates graft-versus-leukemia effects and graft-versus-host disease induced by donor CD8 T cells. *Blood* **99**, 4207–4215 (2002).
58. L. P. Wachsmuth, M. T. Patterson, M. A. Eckhaus, D. J. Venzon, R. E. Gress, C. G. Kanakry, Posttransplantation cyclophosphamide prevents graft-versus-host disease by inducing alloreactive T cell dysfunction and suppression. *J. Clin. Investig.* **129**, 2357–2373 (2019).
59. L. P. Wachsmuth, M. T. Patterson, M. A. Eckhaus, D. J. Venzon, C. G. Kanakry, Optimized timing of post-transplantation cyclophosphamide in MHC-haploidentical murine hematopoietic cell transplantation. *Biol. Blood Marrow Transplant.* **26**, 230–241 (2020).
60. E. Brissot, M. Labopin, G. Ehninger, M. Stelljes, A. Brecht, A. Ganser, J. Tischer, N. Kröger, B. Afanasyev, J. Finke, A. Elmaagacli, H. Einsele, M. Mohty, A. Nagler, Haploidentical versus unrelated allogeneic stem cell transplantation for relapsed/refractory acute myeloid leukemia: A report on 1578 patients from the Acute Leukemia Working Party of the EBMT. *Haematologica* **104**, 524–532 (2019).
61. S. O. Ciurea, M. J. Zhang, A. A. Bacigalupo, A. Bashey, F. R. Appelbaum, O. S. Aljitawi, P. Armand, J. H. Antin, J. Chen, S. M. Devine, D. H. Fowler, L. Luznik, R. Nakamura, P. V. O'Donnell, M. A. Perales, S. R. Pingali, D. L. Porter, M. R. Riches, O. T. Ringdén, V. Rocha, R. Vij, D. J. Weisdorf, R. E. Champlin, M. M. Horowitz, E. J. Fuchs, M. Eapen, Haploidentical transplant with posttransplant cyclophosphamide vs matched unrelated donor transplant for acute myeloid leukemia. *Blood* **126**, 1033–1040 (2015).
62. S. R. McCurdy, Y. L. Kasamon, C. G. Kanakry, J. Bolaños-Meade, H. L. Tsai, M. M. Showel, J. A. Kanakry, H. J. Symons, I. Gojo, B. D. Smith, M. P. Bettinotti, W. H. Matsui, A. E. Dezern, C. A. Huff, I. Borrello, K. W. Pratz, D. E. Gladstone, L. J. Swinnen, R. A. Brodsky, M. J. Levis, R. F. Ambinder, E. J. Fuchs, G. L. Rosner, R. J. Jones, L. Luznik, Comparable composite endpoints after HLA-matched and HLA-haploidentical transplantation with post-transplantation cyclophosphamide. *Haematologica* **102**, 391–400 (2017).
63. A. Rashidi, M. Hamadani, M.-J. Zhang, H.-L. Wang, H. Abdel-Azim, M. Aljurf, A. Assal, A. Bajel, A. Bashey, M. Battiwalla, A. M. Beitinjaneh, N. Bejanyan, V. R. Bhatt, J. Bolaños-Meade, M. Byrne, J.-Y. Cahn, M. Cairo, S. Ciurea, E. Copelan, C. Cutler, A. Daly, M.-A. Diaz, N. Farhadfar, R. P. Gale, S. Ganguly, M. R. Grunwald, T. Hahn, S. Hashmi, G. C. Hildebrandt, H. K. Holland, N. Hossain, C. G. Kanakry, M. A. Kharfan-Dabaja, N. Khera, Y. Koc, H. M. Lazarus, J.-W. Lee, J. Maertens, R. Martino, J. McGuirk, R. Munker, H. S. Murthy, R. Nakamura, S. Nathan, T. Nishihori, N. Palmisiano, S. Patel, J. Pidala, R. Olin, R. F. Olsson, B. Oran, O. Ringden, D. Rizzieri, J. Rowe, M. L. Savoie, K. R. Schultz, S. Seo, B. C. Shaffer, A. Singh, M. Solh, K. Stockerl-Goldstein, L. F. Verdonck, J. Wagner, E. K. Waller, M. De Lima, B. M. Sandmaier, M. Litzow, D. Weisdorf, R. Romee, W. Saber, Outcomes of haploidentical vs matched sibling transplantation for acute myeloid leukemia in first complete remission. *Blood Adv.* **3**, 1826–1836 (2019).
64. S. R. McCurdy, V. Radojcic, H. L. Tsai, A. Vulic, E. Thompson, S. Ivcevic, C. G. Kanakry, J. D. Powell, B. Lohman, D. Adom, S. Paczesny, K. R. Cooke, R. J. Jones, R. Varadhan, H. J. Symons, L. Luznik, Signatures of GVHD and relapse after posttransplant cyclophosphamide revealed by immune profiling and machine learning. *Blood* **139**, 608–623 (2022).
65. K. Bartsch, H. Al-Ali, A. Reinhardt, C. Franke, M. Hudecek, M. Kamprad, S. Tschiedel, M. Cross, D. Niederwieser, C. Gentilini, Mesenchymal stem cells remain host-derived independent of the source of the stem-cell graft and conditioning regimen used. *Transplantation* **87**, 217–221 (2009).
66. S. O. Ciurea, J. R. Schafer, R. Bassett, C. J. Denman, K. Cao, D. Willis, G. Rondon, J. Chen, D. Soebbing, I. Kaur, A. Gulbis, S. Ahmed, K. Rezvani, E. J. Shpall, D. A. Lee, R. E. Champlin, Phase 1 clinical trial using mbIL21 ex vivo-expanded donor-derived NK cells after haploidentical transplantation. *Blood* **130**, 1857–1868 (2017).
67. C. Van Elssen, S. O. Ciurea, NK cell alloreactivity in acute myeloid leukemia in the post-transplant cyclophosphamide era. *Am. J. Hematol.* **95**, 1590–1598 (2020).
68. M. Chesi, D. F. Robbiani, M. Sebag, W. J. Chng, M. Affer, R. Tiedemann, R. Valdez, S. E. Palmer, S. S. Haas, A. K. Stewart, R. Fonseca, R. Kremer, G. Cattoretti, P. L. Bergsagel, AID-dependent activation of a MYC transgene induces multiple myeloma in a conditional mouse model of post-germinal center malignancies. *Cancer Cell* **13**, 167–180 (2008).
69. M. Chesi, G. M. Matthews, V. M. Garbitt, S. E. Palmer, J. Shortt, M. Lefebure, A. K. Stewart, R. W. Johnstone, P. L. Bergsagel, Drug response in a genetically engineered mouse model of multiple myeloma is predictive of clinical efficacy. *Blood* **120**, 376–385 (2012).
70. K. A. Markey, R. D. Kuns, D. J. Browne, K. H. Gartlan, R. J. Robb, J. P. Martins, A. S. Henden, S. A. Minnie, M. Cheong, M. Koyama, M. J. Smyth, R. J. Steptoe, G. T. Belz, T. Brocker, M. A. Degli-Esposti, S. W. Lane, G. R. Hill, Flt-3L expansion of recipient $CD8\alpha^+$ dendritic cells deletes alloreactive donor t cells and represents an alternative to posttransplant cyclophosphamide for the prevention of GVHD. *Clin. Cancer Res.* **24**, 1604–1616 (2018).
71. S. W. Lane, Y. J. Wang, C. Lo Celso, C. Ragu, L. Bullinger, S. M. Sykes, F. Ferraro, S. Shterental, C. P. Lin, D. G. Gilliland, D. T. Scadden, S. A. Armstrong, D. A. Williams, Differential niche and Wnt requirements during acute myeloid leukemia progression. *Blood* **118**, 2849–2856 (2011).
72. K. A. Markey, A. C. Burman, T. Banovic, R. D. Kuns, N. C. Raffelt, V. Rowe, S. D. Olver, A. L. Don, E. S. Morris, A. R. Pettit, Y. A. Wilson, R. J. Robb, L. M. Randall, H. Korner, C. R. Engwerda, A. D. Clouston, K. P. Macdonald, G. R. Hill, Soluble lymphotoxin is an important effector molecule in GVHD and GVL. *Blood* **115**, 122–132 (2010).
73. K. R. Cooke, L. Kobzik, T. R. Martin, J. Brewer, J. Delmonte Jr., J. M. Crawford, J. L. Ferrara, An experimental model of idiopathic pneumonia syndrome after bone marrow transplantation: I. The roles of minor H antigens and endotoxin. *Blood* **88**, 3230–3239 (1996).
74. J. Feng, T. Liu, B. Qin, Y. Zhang, X. S. Liu, Identifying ChIP-seq enrichment using MACS. *Nat. Protoc.* **7**, 1728–1740 (2012).
75. T. Stuart, A. Srivastava, C. Lareau, R. Satija, Multimodal single-cell chromatin analysis with Signac. bioRxiv 2020.11.09.373613 [Preprint]. 10 November 2020. https://doi.org/10.1101/2020.11.09.373613.
76. C. Hafemeister, R. Satija, Normalization and variance stabilization of single-cell RNA-seq data using regularized negative binomial regression. *Genome Biol.* **20**, 296 (2019).
77. C. Ahlmann-Eltze, W. Huber, glmGamPoi: Fitting Gamma-Poisson generalized linear models on single cell count data. *Bioinformatics* **36**, 5701–5702 (2021).
78. Y. Hao, S. Hao, E. Andersen-Nissen, W. M. Mauck III, S. Zheng, A. Butler, M. J. Lee, A. J. Wilk, C. Darby, M. Zager, P. Hoffman, M. Stoeckius, E. Papalexi, E. P. Mimitou, J. Jain, A. Srivastava, T. Stuart, L. M. Fleming, B. Yeung, A. J. Rogers, J. M. McElrath, C. A. Blish, R. Gottardo,

P. Smibert, R. Satija, Integrated analysis of multimodal single-cell data. *Cell* **184**, 3573–3587.e29 (2021).
79. A. N. Schep, B. Wu, J. D. Buenrostro, W. J. Greenleaf, chromVAR: Inferring transcription-factor-associated accessibility from single-cell epigenomic data. *Nat. Methods* **14**, 975–978 (2017).

Acknowledgments: We thank the Fred Hutch Vaccine and Infectious Disease Division for the support of the peripheral blood mononuclear cell biorepository. **Funding:** S.A.M. is funded by a Klorfine fellowship and ASTCT New Investigator Award. D.Z. is funded by a K23 award (1K23AI163343-01A1). This work was supported by an NIH/NCI P01 award (CA078902). **Author contributions:** S.A.M. designed and performed experiments, analyzed data, and wrote the manuscript. O.G.W. analyzed data. N.S.N., K.S.E., C.R.S., G.C., S.S.B., S.W.L., L.D.S., and R.D.K. performed experiments. K.A.M., M.K., A.Y., and S.V. assisted with data interpretation and experimental design. T.Z., J.D.H., S.R.W.L., D.Z., A.S., M.B., and A.M.R. provided reagents and/or interpreted data. S.N.F. analyzed and interpreted data. G.R.H. conceived the study and wrote the manuscript. All authors edited and approved the final manuscript. **Competing interests:** S.A.M., G.R.H., and A.M.R. have filed a provisional patent application on the use of DR-18 in hematological malignancies. G.R.H. has consulted for Generon Corporation, NapaJen Pharma, iTeos Therapeutics, and Neoleukin Therapeutics and has received research funding from Compass Therapeutics, Syndax Pharmaceuticals, Applied Molecular Transport, Serplus Technology, Heat Biologics, Laevoroc Oncology, and iTeos Therapeutics. K.A.M. is on the scientific advisory board for Postbiotics Plus. S.W.L. is on the advisory board for Janssen, Astellas, Celgene/BMS, and Novartis and has received research funding from Janssen, Celgene/BMS, and a speaker's honorarium from AbbVie. A.M.R. is on the board of directors, has consulted for, has ownership interest and intellectual property in, and has received research funding from Simcha Therapeutics, the commercial licensee of the DR-18 program. A.S. is on the advisory board for BMS, Janssen, Secura Bio, AbbVie, Haemalogix, Pfizer, Roche, Amgen, and Antegene. A.S. received speaker's bureau from BMS and Janssen; research support from BMS, Janssen, Amgen, Haemalogix, AbbVie, and PharmaMar; and honoraria from BMS, Janssen, Amgen, Secura Bio, AbbVie, Haemalogix, Pfizer, Roche, and Antegene. All other authors declare that they have no competing interests. **Data and materials availability:** New RNA sequencing data are available at the Gene Expression Omnibus (GEO) repository under accession number GSE211464. DR-18 was provided by Simcha Therapeutics under a materials transfer agreement, and requests for access should be addressed to A.M.R. (aaron.ring@yale.edu). All other data needed to evaluate the conclusions in the paper are present in the paper or the Supplementary Materials.

Submitted 28 January 2022
Accepted 19 September 2022
Published 14 October 2022
10.1126/sciimmunol.abo3420

Science Immunology

Depletion of exhausted alloreactive T cells enables targeting of stem-like memory T cells to generate tumor-specific immunity

Simone A. Minnie, Olivia G. Waltner, Kathleen S. Ensbey, Nicole S. Nemychenkov, Christine R. Schmidt, Shruti S. Bhise, Samuel R. W. Legg, Gabriela Campoy, Luke D. Samson, Rachel D. Kuns, Ting Zhou, John D. Huck, Slavica Vuckovic, Danniel Zamora, Albert Yeh, Andrew Spencer, Motoko Koyama, Kate A. Markey, Steven W. Lane, Michael Boeckh, Aaron M. Ring, Scott N. Furlan, and Geoffrey R. Hill

Sci. Immunol., **7** (76), eabo3420.
DOI: 10.1126/sciimmunol.abo3420

Flipping the switch on graft-versus-tumor effects

Allogeneic bone marrow transplantation (alloBMT) is a potentially curative treatment for hematological malignancies but is prone to tumor relapse due to escape from graft-versus-tumor (GVT) effects, especially when accompanied by systemic immunosuppression. Using a mouse model of myeloma resistant to treatment with alloBMT, Minnie *et al.* found that alloBMT-derived donor T cells become functionally exhausted from exposure to alloantigen rather than tumor antigen. Post-transplant cyclophosphamide depleted alloantigen-driven exhausted T cells, leaving a population bearing a stem cell memory–like gene signature. In leukemia-bearing mice receiving a haploidentical transplant, agonist immunotherapy with an engineered IL-18 resistant to endogenous inhibitors enhanced the antitumor immunity and improved survival. These results demonstrate that immunotherapy targeting residual T cell populations can improve the GVT response of alloBMT during systemic immunosuppression.